

## REPORT No. 849

# THE EFFECT OF WALL INTERFERENCE UPON THE AERODYNAMIC CHARACTERISTICS OF AN AIRFOIL SPANNING A CLOSED-THROAT CIRCULAR WIND TUNNEL

By WALTER G. VINCENTI and DONALD J. GRAHAM

### SUMMARY

*The results of a theoretical and experimental investigation of wall interference for an airfoil spanning a closed-throat circular wind tunnel are presented. Analytical equations are derived which relate the characteristics of an airfoil in the tunnel at subsonic speeds with the characteristics in free air. The analysis takes into consideration the effect of fluid compressibility and is based upon the assumption that the chord of the airfoil is small as compared with the diameter of the tunnel. The development is restricted to an untwisted, constant-chord airfoil spanning the middle of the tunnel. Brief theoretical consideration is also given to the problem of choking at high speeds. Results are then presented of tests to determine the low-speed characteristics of an NACA 4412 airfoil for two chord-diameter ratios. While, on the basis of these experiments, no appraisal is possible of the accuracy of the corrections at high speeds, the data indicate that at low Mach numbers the analytical results are valid, even for relatively large values of the chord-diameter ratio.*

### INTRODUCTION

The design of modern high-performance airplanes requires, insofar as possible, an accurate knowledge of airfoil profile data at Reynolds and Mach numbers attained in flight. Since the size and power of wind tunnels are subject to various practical limitations, most existing tunnels, even if they can provide the desired Mach number, are not capable of attaining full-scale Reynolds numbers for all flight conditions. To minimize this shortcoming in tunnel tests of airfoil profiles, it is therefore necessary to use models having as large a chord as possible relative to the cross-sectional dimensions of the tunnel test section. In order to eliminate the effects of supporting struts and to exclude the indeterminate tunnel-boundary interference involved in the testing of large-chord airfoils of limited span, it has become common practice in such tests to use airfoils which completely span the test section. Even for these so-called "through" models, however, the tunnel-boundary interference can still be considerable, and accurate correction must be made for its effects if the tunnel data are to be used with confidence in the calculation of free-flight airplane characteristics.

The tunnel-boundary interference for airfoils spanning wind tunnels of various types has been the subject of numerous theoretical and experimental investigations. The interference for rectangular tunnels having rigid walls normal to the span of the airfoil and either rigid walls or free boundaries

parallel to the span has been discussed theoretically by several writers. For example, Lock (reference 1), Glauert (reference 2), and Goldstein (reference 3), give the necessary tunnel-wall corrections for an airfoil spanning a rectangular tunnel in an incompressible fluid; while Goldstein and Young (reference 4) show how these corrections, as well as those for any general case of interference in an incompressible fluid, can be modified to take account of fluid compressibility. Reference 5 gives the corrections for the compressible case in a closed-throat rectangular tunnel, as well as a critical discussion of the results of the previous references and some experimental data from low-speed tests. Fage (reference 6) also presents experimental drag data for several symmetrical bodies of various sizes in a closed-throat rectangular tunnel. Experimental and theoretical results for an airfoil spanning a completely open-throat rectangular tunnel are given by Stüper (references 7 and 8). The case of an airfoil spanning an open-throat circular tunnel has been the subject of a number of investigations, including theoretical treatments by Glauert (reference 9), Stüper (references 7 and 8), and Squire (reference 10), and experimental measurements by Stüper (references 7 and 8) and Adamson (reference 11). Apparently, the case of the closed-throat circular tunnel has received no attention.

Since this last case is often encountered in practice, an investigation was made of the tunnel-wall interference at subsonic speeds for a wing spanning a closed-throat circular tunnel. The present paper presents the results of this investigation. In the first part of the paper, analytical equations are derived relating the characteristics of the airfoil in the tunnel with those in free air for a compressible fluid. Some consideration is also given to the phenomenon of choking which occurs at high speeds. In the second part, the validity of the theoretical results is examined by the analysis of experimental data for an NACA 4412 airfoil for two ratios of airfoil chord to tunnel diameter. The investigation is restricted to untwisted constant-chord airfoils spanning the middle of the tunnel.

### THEORY

As in reference 5, the theoretical development of the tunnel-wall corrections is divided conveniently into two general sections. First, the influence of the wall upon the field of flow at the airfoil in the tunnel is determined. Second, the aerodynamic characteristics of the airfoil in this field of flow are related to the corresponding quantities in free air.

In this manner, simple formulas are finally obtained which enable the prediction of the free-air characteristics when the characteristics in the tunnel are known.

Again, as in reference 5, the analysis is based upon the method of superposition. To this end, it is assumed that the airfoil is of small thickness and camber, so that the induced velocity is everywhere small as compared with the velocity of the undisturbed stream. With this assumption, the total induced velocity at any point is the simple vector sum of the separate velocities induced at that point by the interference between the tunnel wall and the airfoil camber, thickness, and wake. Thus the effects of camber, thickness, and wake may each be analyzed separately and superposed to obtain the desired result for the complete airfoil. As pointed out in reference 5, this procedure is permissible even in the compressible fluid if the airfoil is of small thickness and camber as assumed.

Before proceeding to the actual development of the theory, it is useful to contrast the present problem with the problems of through airfoils in the various types of rectangular tunnels and in the open-throat circular tunnel. In the case of an airfoil spanning a rectangular tunnel having rigid walls normal to the span of the airfoil, the problem is relatively simple. If the effect of the boundary layer along the tunnel walls is neglected, the flow is sensibly the same in all planes normal to the span; that is, there is clearly no spanwise variation in lift. The air flow is thus essentially two-dimensional, and the interference problems of camber, thickness, and wake can be analyzed by the customary means of a system of images with axes parallel to the span of the airfoil (references 1, 2, 3, and 5). This is true whether the tunnel boundaries parallel to the span are fixed or free. In this manner, tunnel-boundary corrections can be derived for airfoils of moderately large chord as compared with the height of the tunnel test section.

In the case of an airfoil spanning a completely free jet, whether rectangular or circular in section, the lift necessarily falls to zero at the boundary of the jet. There thus exists in this case a pronounced spanwise variation in lift and an attendant system of trailing vortices. In the existing treatments of the problem, only the interference between these trailing vortices and the jet boundaries is considered, the interference effects associated with the chordwise distribution of bound vortices and with the airfoil thickness and wake being completely neglected. This procedure implies the assumption that the chord of the airfoil is very small relative to the dimensions of the jet. In this manner, the problem is reduced to a limiting case of the usual problem of an airfoil partially spanning the jet, and, as in this latter case, the component of downwash induced at the airfoil by the interference between the walls and the trailing vortices is one-half as great as the corresponding component an infinite distance downstream. The theoretical determination of the wall interference may thus be treated as a problem of two-dimensional flow in a plane normal to the axis of the tunnel infinitely far behind the airfoil. The boundary conditions for either the rectangular or circular jet are then readily satisfied by the introduction of a suitable system of image vortices with axes parallel to the axis of the tunnel

(references 7, 8, 9, and 10). This method of analysis, however, is inadequate if the chord of the airfoil is even moderately large as compared with the dimensions of the jet.

The case of the airfoil spanning a closed-throat circular tunnel is more complex than either of the foregoing problems. Unlike the condition prevailing in the free jet, the lift in this case need not fall to zero at the boundary—that is, at the tunnel wall—so that the spanwise variation in lift is not necessarily large. In fact, as will be seen, the lift is constant across the span of the airfoil, and no system of trailing vortices exists. The assumption of a very small chord and the consequent reduction of the problem to a case of two-dimensional flow in a plane infinitely far downstream is thus without meaning. On the other hand, an analysis for airfoils of moderately large chord in the manner employed in the case of the rectangular tunnel with rigid side walls is not possible. In the closed-throat circular tunnel the flow in all planes normal to the span of the airfoil is not the same, so that the effect of the bound vortices, and of the airfoil thickness and wake as well, cannot be treated as a problem in two-dimensional flow. Furthermore, the boundary conditions at the tunnel wall cannot be satisfied for the actual three-dimensional problem by any known system of images. The solution of the problem for the closed-throat circular tunnel thus requires an analysis entirely different from those employed in the previous instances.

#### INFLUENCE OF TUNNEL WALL UPON FIELD OF FLOW AT AIRFOIL

An approach to the problem of the airfoil spanning a closed-throat circular tunnel is afforded by the work of von Kármán and Burgers in reference 12 (pp. 266 to 273), where the velocity potential at an arbitrary point in the tunnel is determined for a U-shape vortex of infinitesimal span in an incompressible fluid.

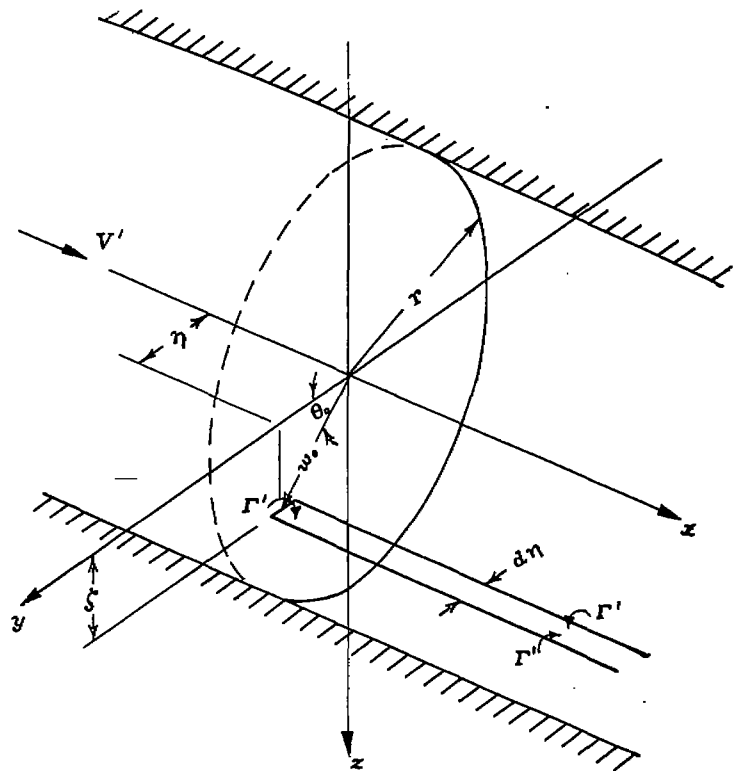


FIGURE 1.—Elementary U-shaped vortex in closed-throat circular tunnel.

A system of rectangular coordinates  $x, y, z$  is introduced as shown in figure 1. The  $x$ -axis is taken on the center line of the tunnel with its positive direction downstream. The  $z$ -axis is positive downward, and the  $y$ -axis positive to the left for an observer looking against the direction of flow. An alternative system of cylindrical coordinates  $x, \omega, \theta$  is defined by the relations

$$\left. \begin{aligned} y &= \omega \cos \theta \\ z &= \omega \sin \theta \end{aligned} \right\} \quad (1)$$

The positive direction of circulation is defined so that a vortex with positive circulation exerts a force on the fluid in the direction of the positive  $z$ -axis. In other words, the lift force experienced by a positive vortex is in the negative  $z$  direction. The velocity of the fluid in the undisturbed stream is denoted by  $V'$  and the radius of the tunnel by  $r$ . Other symbols are defined as introduced in the text. A list of the more important symbols and their definitions is given in Appendix C.

Consider now a U-shape vortex of infinitesimal span  $d\eta$  parallel to the  $y$ -axis and situated in the  $yz$ -plane at the point  $\eta = \omega_0 \cos \theta_0, \zeta = \omega_0 \sin \theta_0$ . If the strength of the vortex is denoted by  $\Gamma'$  the velocity potential in the closed tunnel at the points  $x, \omega, \theta$  is given by von Kármán and Burgers, for negative values of  $x$ , as

$$\phi = -\frac{\Gamma' d\eta}{4\pi} \int_0^\infty \frac{\partial \Omega}{\partial \xi} d\xi \quad (2)$$

where

$$\Omega = \frac{4}{r^2} \sum_{m=0}^{\infty} \sum_{s=1}^{\infty} \cos m(\theta - \theta_0) e^{-\lambda_s(\xi - x)} \left[ \frac{J_m(\lambda_s \omega) J_m(\lambda_s \omega_0)}{\left(1 - \frac{m^2}{\lambda_s^2 r^2}\right) \lambda_s J_m^2(\lambda_s r)} \right] - \frac{2(\xi - x)}{r^2} \quad (3)$$

(It should be noted that the quantity  $\xi$  appearing in these equations is merely a variable of integration and has no physical significance.) The quantity  $J_m(\lambda_s \omega)$  is a Bessel function of the first kind of the order  $m$ . The summation with respect to  $m$  extends over all the positive integers and includes  $m=0$ ; the prime added to the summation sign indicates that a factor  $\frac{1}{2}$  must be inserted before the term corresponding to  $m=0$ . The summation with respect to  $s$  for every  $m$  extends over all positive roots of the equation

$$J_m'(\lambda_s r) = 0 \quad (4)$$

where  $J_m'(\lambda_s r)$  is the derivative of the function  $J_m(\lambda_s r)$  with respect to its argument. The notation used throughout this paper for the Bessel functions is that of Watson (reference 13), which is the same as that of the Smithsonian tables (reference 14).

By differentiating  $\Omega$  with respect to  $\zeta$  and then integrating with respect to  $\xi$ , as indicated in equation (2), the velocity potential becomes finally

$$\phi = -\frac{\Gamma' d\eta}{\pi r^2} \sum_{m=0}^{\infty} \sum_{s=1}^{\infty} \frac{e^{\lambda_s x} J_m(\lambda_s \omega)}{\left(1 - \frac{m^2}{\lambda_s^2 r^2}\right) \lambda_s^2 J_m^2(\lambda_s r)} \times \left[ m \cos \theta_0 \sin m(\theta - \theta_0) \frac{J_m(\lambda_s \omega_0)}{\omega_0} + \lambda_s \sin \theta_0 \cos m(\theta - \theta_0) J_m'(\lambda_s \omega_0) \right] \quad (5)$$

As pointed out, this expression applies only at negative values of  $x$ . As will be seen later, the necessary results for positive values of  $x$  can be derived from considerations of symmetry.

By means of equation (5), it is possible to evaluate the wall interference associated with both airfoil camber and thickness for the case of the incompressible fluid. These results can then be modified for the effect of fluid compressibility by the methods of reference 4. It is found finally that, for a closed-throat circular tunnel, the effects of interference between the walls and the airfoil camber are identical with the corresponding interference effects for the same airfoil spanning a closed-throat rectangular tunnel, the height of which bears a known relation to the diameter of the circular tunnel. A similar conclusion is obtained regarding the effects of interference between the walls and the airfoil thickness, except for a numerical difference in the relation between the diameter of the given circular tunnel and the height of the equivalent rectangular tunnel. The interference effects associated with the wake of the airfoil are not analyzed in detail, but their magnitude can be estimated with reasonable accuracy by comparison with the results for the thickness effect. In order to simplify the complex mathematics of the problem, the interference effects are calculated only for the section of the airfoil at the center line of the tunnel. As will be seen later, however, experimental data indicate that the results are applicable at any spanwise station.

**Camber effect.**—To analyze the effect of the interference between the tunnel walls and the airfoil camber, the thickness and wake of the airfoil are considered to be removed and the airfoil reduced to its mean camber line. The resulting infinitesimally thin airfoil may then be replaced by a sheet of continuously distributed, bound vortices which, in the general three-dimensional case, consist of both spanwise and chordwise vortices. The velocity induced at any given point on the camber line is then obtained by integration over the entire vortex sheet. As in all thin-airfoil theory the distribution of bound vorticity must be such that the resultant of this induced velocity and the free-stream velocity is tangential to the camber line at all points. As will be seen, however, the actual theoretical determination of the distribution of vorticity is not necessary in this case.

In calculating the velocity field of the vortex system, it is assumed that the bound vorticity is distributed in the middle plane of the tunnel—that is, in the  $xy$ -plane—rather than along the camber line and that the induced velocity at any point on the camber line is the same as the induced velocity at the corresponding point in the  $xy$ -plane. From equation

(5), the velocity potential at any point  $x, \omega, \theta$  for a vortex element on the  $y$ -axis at the point  $y=\eta$  ( $\theta_0=0, \omega_0=\eta$ ) is

$$\phi = -\frac{\Gamma'd\eta}{\pi r^2} \sum_{m=1}^{\infty} \sum_{s=1}^{\infty} \frac{m \sin m\theta e^{\lambda_s x} J_m(\lambda_s \omega) J_m(\lambda_s \eta)}{\eta \left(1 - \frac{m^2}{\lambda_s^2 r^2}\right) \lambda_s^2 J_m^2(\lambda_s r)} \quad (6)$$

The term for  $m=0$  disappears by virtue of the factor  $m$  in the numerator of the general term. The vertical induced velocity  $v_z'$  in the incompressible fluid is then

$$v_z' = \frac{\partial \phi}{\partial z} = \frac{\partial \phi}{\partial \theta} \frac{\partial \theta}{\partial z} + \frac{\partial \phi}{\partial \omega} \frac{\partial \omega}{\partial z}$$

For points in the  $xy$ -plane ( $\theta=0, \omega=y$ ),  $\frac{\partial \omega}{\partial z}=0$  and  $\frac{\partial \theta}{\partial z} = \frac{1}{y}$ .

Thus, at points in the  $xy$ -plane,

$$v_z' = -\frac{\Gamma'd\eta}{\pi r^2} \sum_{m=1}^{\infty} \sum_{s=1}^{\infty} \frac{m^2 e^{\lambda_s x} J_m(\lambda_s y) J_m(\lambda_s \eta)}{\eta y \left(1 - \frac{m^2}{\lambda_s^2 r^2}\right) \lambda_s^2 J_m^2(\lambda_s r)} \quad (7)$$

The complicated double series in this equation can be reduced to a single series and the mathematics of the problem greatly simplified by limiting the discussion to the chordwise section of the airfoil at the center line of the tunnel ( $y=0, z=0$ ). From the known relations for Bessel functions (cf. reference 13), for  $y=0$

$$\frac{J_1(\lambda_s y)}{\lambda_s y} = 1/2$$

$$\frac{J_m(\lambda_s y)}{\lambda_s y} = 0 \text{ for } m > 1$$

Thus, at points on the  $x$ -axis,

$$v_z' = -\frac{\Gamma'd\eta}{2\pi r^2} \sum_{s=1}^{\infty} \frac{e^{\lambda_s x} J_1(\lambda_s \eta)}{\eta \left(1 - \frac{1}{\lambda_s^2 r^2}\right) \lambda_s J_1^2(\lambda_s r)} \quad (8)$$

where the summation with respect to  $s$  extends over all the positive roots of the equation

$$J_1'(\lambda_s r) = 0 \quad (9)$$

From Bessel's differential equation

$$J_1''(\lambda_s r) = -\left(1 - \frac{1}{\lambda_s^2 r^2}\right) J_1(\lambda_s r) \quad (10)$$

where the double prime denotes the second derivative of the Bessel function with respect to its argument. Equation (8) can thus be written

$$v_z' = \frac{\Gamma'd\eta}{2\pi r\eta} \sum_{s=1}^{\infty} \frac{e^{\lambda_s x} J_1(\lambda_s \eta)}{\lambda_s r J_1(\lambda_s r) J_1''(\lambda_s r)} \quad (11)$$

As mentioned, this equation is valid only for negative values of  $x$ .

It is apparent that the series in equation (11) is rapidly convergent for large negative values of  $x$ , but that the convergence is slow for small negative values. Since in the evaluation of the velocity induced by the vortex sheet it

is the small values of  $x$  which are of primary importance, equation (11) cannot be applied directly in the present case. It is possible, however, by means of a method demonstrated by Watson (reference 15), to express the series of this equation as a combination of elementary functions and a series of ascending powers of  $x$  and  $\eta$ . The resulting series is readily applicable to the present problem.

The detailed procedure for the transformation of the series of equation (11) is given in Appendix A. By application of the final result, equation (11) may be written.

$$v_z' = \frac{\Gamma'd\eta}{2\pi r\eta} \sum_{s=1}^{\infty} \frac{e^{\lambda_s x} J_1(\lambda_s \eta)}{\lambda_s r J_1(\lambda_s r) J_1''(\lambda_s r)} = \frac{\Gamma'd\eta}{2\pi r\eta} \left[ -\frac{r^2 + \eta^2}{2r\eta} - \frac{rx}{2\eta\sqrt{\eta^2 + x^2}} + \sum_{k=0}^{\infty} \sum_{p=0}^{\infty} \frac{(-1)^k \mu'_{2(k+p+1)} \eta^{2k+1} x^{2p+1}}{k!(k+1)!(2p+1)! 2^{2k+1} r^{2(k+p+1)}} \right] \quad (12)$$

The double summation extends over all integral values of  $k$  and  $p$  from zero to positive infinity. The numerical coefficient  $\mu'_{2(k+p+1)} = \mu'_{2f}$  is given by the integral

$$\mu'_{2f} = -\frac{1}{(2f+1)\pi} \int_0^{\infty} \frac{t^{2f-2}(1+t^2)}{[I_1'(t)]^2} dt \quad (13)$$

Here  $I_1(t)$  is a modified Bessel function of the first kind of order unity, and  $I_1'(t)$  denotes the derivative of  $I_1(t)$  with respect to its argument. The numerical values of  $\mu'_{2f}$  for  $f=1, 2, 3, 4$ , are evaluated by means of a series expansion in Appendix A.

It is readily shown that the first term on the right-hand side of equation (12) agrees with the induced velocity computed for  $x=0$  by the more elementary theory of tunnel-wall interference which considers only the effects of the trailing vortices and their images. To this end, consider the two-dimensional flow in a plane normal to the axis of the tunnel an infinite distance downstream (fig. 2). The theory states that the induced velocity at a given point  $(y, z)$  in this plane is twice as great as the induced velocity at the corresponding point in the plane  $x=0$  (cf. reference 12, p. 260). In the plane  $x=\infty$ , the trailing vortices of the U-shape vortex previously considered constitute a vortex pair having an infinitesimal spacing  $d\eta$  and situated at the point  $y=\eta, z=0$ . The circulation of each vortex of the pair is  $\Gamma'$  and is directed as shown

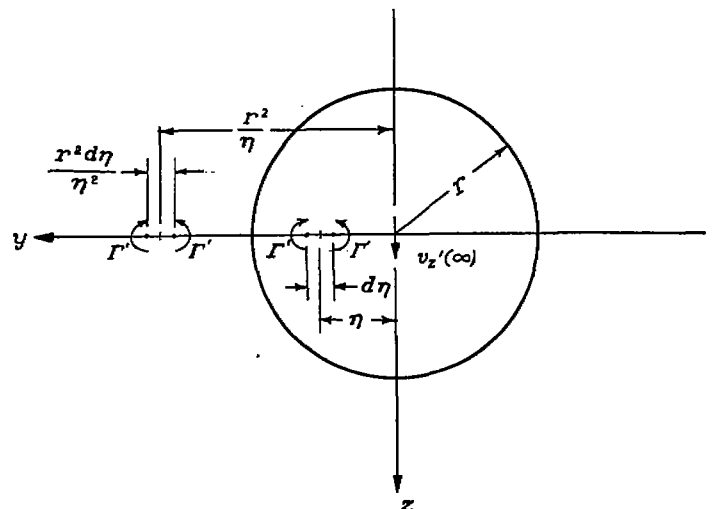


FIGURE 2.—Section through tunnel at infinity downstream.

in figure 2. The boundary condition that there shall be no flow normal to the wall of the tunnel can be satisfied by the introduction at the point  $z=0, y=r^2/\eta$  of an image vortex pair with a spacing  $r^2 d\eta/\eta^2$  and with the circulation of the vortices directed as indicated. The vertical velocity induced at the tunnel center by the trailing vortex pair is

$$v_{s_1}'(\infty) = -\frac{\Gamma' d\eta}{2\pi\eta^2}$$

and the vertical velocity induced at the same point by the image vortex pair is

$$v_{s_2}'(\infty) = -\frac{\Gamma' \frac{r^2 d\eta}{\eta^2}}{2\pi \left(\frac{r^2}{\eta}\right)^2} = -\frac{\Gamma' d\eta}{2\pi r^2}$$

The total vertical velocity at the center of the tunnel at  $x = \infty$  is then the sum of these two velocities; that is,

$$v_s'(\infty) = -\frac{\Gamma' d\eta (r^2 + \eta^2)}{2\pi r^2 \eta^2} \quad (14)$$

The vertical velocity at the center of the tunnel at  $x=0$  is one-half of this value, or

$$v_s'(0) = -\frac{\Gamma' d\eta (r^2 + \eta^2)}{4\pi r^2 \eta^2} \quad (15)$$

This value agrees with the result of equation (12) for the special case  $x=0$ . Thus, the first term on the right-hand side of equation (12) represents the vertical induced velocity on the center line of the tunnel at  $x=0$  and is attributable entirely to the trailing vortices and to the interference between these vortices and the tunnel walls. The remaining terms represent the variation in induced velocity due to a displacement a distance  $x$  upstream from the origin. These terms arise both from a change in the effect of the trailing vortices and their wall interference and from the now-active effect of the transverse bound vortex and its interference with the tunnel walls.

Although equation (12) was deduced for negative values of  $x$ , it can be shown that it is applicable to positive values of  $x$  as well. According to von Kármán and Burgers (reference 12, p. 267), the vertical induced velocity at  $-x$  is related to the corresponding velocity at  $+x$  by the equation

$$v_s'(-x) = v_s'(\infty) - v_s'(+x)$$

By virtue of this relation, together with the fact that

$$v_s'(0) = \frac{1}{2} v_s'(\infty), \text{ it follows that}$$

$$v_s'(x) - v_s'(0) = -[v_s'(-x) - v_s'(0)] \quad (16)$$

That is, the difference between the induced velocity at a given station  $x$  and the induced velocity at  $x=0$  must be an odd function of  $x$ . The terms containing  $x$  in equation (12), which were derived to represent this difference for negative values of the variable, are seen to constitute precisely such a function. Thus the expansion of equation (12) is valid for positive as well as negative values of  $x$ .

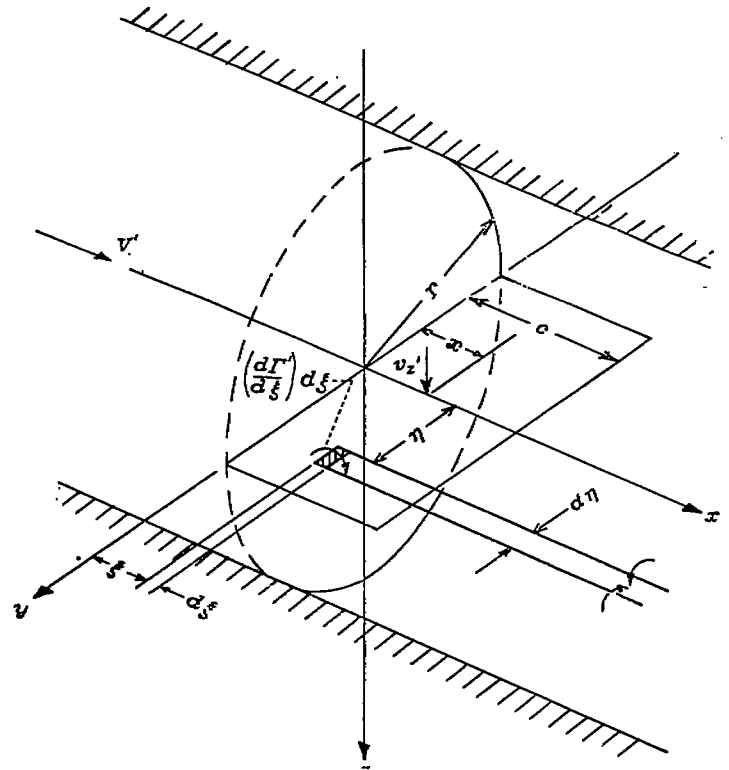


FIGURE 3.—Infinitely thin airfoil spanning closed-throat circular tunnel.

The vortex sheet which represents the entire airfoil can now be built up by the superposition of U-shape vortices in the  $xy$ -plane, and the total induced velocity found by integration of equation (12) over the entire system. The leading edge of the airfoil is placed on the  $y$ -axis as shown in figure 3; the trailing edge then lies at  $x=c$ , where  $c$  is the chord of the airfoil. The circulation of an elementary vortex having an infinitesimal span  $d\eta$  and situated at the point  $x=\xi, y=\eta$  is taken to be  $(d\Gamma'/d\xi)d\xi$ , where  $(d\Gamma'/d\xi)$  is the vorticity per unit length of the chordwise section at the station  $y=\eta$ . The vertical velocity induced at the chordwise station  $x$  on the center line of the tunnel by a single elementary vortex is given by equation (12) if  $x$  and  $\Gamma'$  are replaced by  $(x-\xi)$  and  $(d\Gamma'/d\xi)d\xi$ , respectively. The total vertical velocity induced by the complete airfoil is then given by the double integral

$$v_s' = \frac{1}{4\pi r} \int_0^c \int_{-r}^{+r} \left(\frac{d\Gamma'}{d\xi}\right) \left[ -\frac{r^2 + \eta^2}{r\eta^2} - \frac{r(x-\xi)}{\eta^2 \sqrt{\eta^2 + (x-\xi)^2}} + \sum_{k=0}^{\infty} \sum_{p=0}^{\infty} \frac{(-1)^p \mu'_{2(k+p+1)} \eta^{2k} (x-\xi)^{2p+1}}{k!(k+1)!(2p+1)! 2^{2k} r^{2(k+p+1)}} \right] d\eta d\xi \quad (17)$$

The integration of equation (17) requires a knowledge of  $(d\Gamma'/d\xi)$  as a function of  $\eta$  and  $\xi$ . Theoretically,  $(d\Gamma'/d\xi)$  could be determined from the requirement that the induced vertical velocity at every point on the camber line must be such that the resultant of this velocity and the free-stream velocity is tangential to the camber line. This method of procedure leads, however, to a complicated double integral equation, the solution of which does not appear feasible. Some assumption concerning the distribution of vorticity must therefore be made if the problem is to be solved.

To aid in the choice of a suitable assumption, experiments were carried out to determine the pressure distribution, both chordwise and spanwise, over an airfoil spanning a closed-throat circular tunnel. The airfoil used in the experiments, which are described in detail later in the report, had an NACA 4412 section and was untwisted and of constant chord. The results of these experiments reveal that for such an arrangement the lift is sensibly uniform across the span for angles of attack below the stall. This fact is illustrated in figures 6 and 7, which show the experimental spanwise lift distribution for the airfoil at various angles of attack in wind tunnels affording chord-diameter ratios of 0.357 and 0.625. These results were at first regarded as rather surprising. Later, however, it was realized that they are only what might logically be expected from general considerations of the conditions of flow in a closed-throat tunnel. A demonstration of this fact is given in Appendix B, in which it is shown that the lift distribution is uniform across an untwisted, constant-chord airfoil spanning any closed-throat wind tunnel, irrespective of the cross-sectional shape of the tunnel. Detailed examination of the pressure distributions from which the results of figures 6 and 7 were obtained reveal further that at a given angle of attack the chordwise pressure distribution is sensibly the same for all spanwise stations on the airfoil; that is, the lift per unit chord at any given chordwise station is constant across the span. It is to be expected that this result, though obtained for a particular airfoil, will be equally true for any ordinary camber-line shape. Thus it is reasonable to assume that the dis-

tribution of bound vorticity is not a function of the spanwise position on the airfoil; that is,  $(d\Gamma'/d\xi)$  is independent of  $\eta$ .

On the basis of this assumption, equation (17) may be written

$$v_z' = \frac{1}{4\pi r} \int_0^c \left( \frac{d\Gamma'}{d\xi} \right) \int_{-r}^{+r} \left[ -\frac{r^2 + \eta^2}{r\eta^2} - \frac{r(x-\xi)}{\eta^2 \sqrt{\eta^2 + (x-\xi)^2}} \right] + \sum_{k=0}^{\infty} \sum_{p=0}^{\infty} \frac{(-1)^p \mu'_{2(k+p+1)} \eta^{2k} (x-\xi)^{2p+1}}{k!(k+1)!(2p+1)!2^{2k-1}(k+p+1)} d\eta d\xi \quad (18)$$

and the integration carried out with respect to  $\eta$ . The first two terms of the integrand, however, become infinite at the point  $\eta=0$ . These singularities, which are due to the effects of the vortices trailing from the vortex elements on the  $x$ -axis, require that special care be taken in the integration. The evaluation of the integral must be carried out from  $-r$  to  $-\epsilon$  and from  $+\epsilon$  to  $+r$ , and to the resulting function must be added the effects of the trailing vortex pairs of span  $2\epsilon$  which straddle the  $x$ -axis. The limit of this sum must then be taken as  $\epsilon$  tends to zero. The vertical velocity induced at the point  $x$  on the  $x$ -axis by the vortices trailing from a vortex element of span  $2\epsilon$  symmetrically placed at  $x=\xi, y=0$  is

$$v_z' = \frac{1}{4\pi} \left( \frac{d\Gamma'}{d\xi} \right) \left[ \frac{2}{\epsilon} + \frac{2(x-\xi)}{\epsilon \sqrt{\epsilon^2 + (x-\xi)^2}} \right] d\xi$$

Since the first two terms of equation (18) contain only second-order powers of  $\eta$ , the integrals from  $-r$  to  $-\epsilon$  and from  $+\epsilon$  to  $+r$  will be equal. The integral of these two terms with respect to  $\eta$  thus becomes finally

$$\int_{-r}^{+r} \left[ -\frac{r^2 + \eta^2}{r\eta^2} - \frac{r(x-\xi)}{\eta^2 \sqrt{\eta^2 + (x-\xi)^2}} \right] d\eta = \lim_{\epsilon \rightarrow 0} \left\{ 2 \int_{+\epsilon}^{+r} \left[ -\frac{r^2 + \eta^2}{r\eta^2} - \frac{r(x-\xi)}{\eta^2 \sqrt{\eta^2 + (x-\xi)^2}} \right] d\eta + 2 \left[ \frac{r}{\epsilon} + \frac{r(x-\xi)}{\epsilon \sqrt{\epsilon^2 + (x-\xi)^2}} \right] \right\} = 2 \lim_{\epsilon \rightarrow 0} \left\{ \frac{\sqrt{r^2 + (x-\xi)^2}}{(x-\xi)} + \frac{\epsilon}{r} - \frac{r\epsilon}{(x-\xi) \sqrt{\epsilon^2 + (x-\xi)^2}} \right\} = \frac{2 \sqrt{1 + \left( \frac{x-\xi}{r} \right)^2}}{\left( \frac{x-\xi}{r} \right)}$$

The integration with respect to  $\eta$  of the double series in equation (18) presents no difficulty. The expression for  $v_z'$  thus becomes after integration

$$v_z' = \frac{1}{4\pi r} \int_0^c \left( \frac{d\Gamma'}{d\xi} \right) \left[ \frac{2 \sqrt{1 + \left( \frac{x-\xi}{r} \right)^2}}{\left( \frac{x-\xi}{r} \right)} + \sum_{k=0}^{\infty} \sum_{p=0}^{\infty} \frac{(-1)^p \mu'_{2(k+p+1)} (x-\xi)^{2p+1}}{k!(k+1)!(2p+1)!(2k+1)2^{2k-1}} \right] d\xi \quad (19)$$

For constant spanwise circulation, the trailing vortices finally disappear in the integration with respect to  $\eta$ . The integrand of equation (19) thus represents the increment of vertical velocity induced by an elementary vortex of constant circulation completely spanning the tunnel.

It will now be assumed that the chord of the airfoil is small enough as compared with the dimensions of the wind tunnel that powers of  $(x-\xi)/r$  greater than the first may be neglected in the integrand of equation (19). This is equiva-

lent to assuming that powers of the chord-diameter ratio  $(c/d)$  higher than the second may be neglected in the final equations for the tunnel-wall corrections. The approximation is accomplished by expanding the first term of the integrand in ascending powers of  $(x-\xi)/r$  and discarding all terms containing powers higher than the first and by retaining only the  $p=0$  terms of the double series. This gives for the induced velocity

$$v_z' = \frac{1}{4\pi r} \int_0^c \frac{d\Gamma'}{d\xi} \left\{ \frac{2}{\left( \frac{x-\xi}{r} \right)} + \left( \frac{x-\xi}{r} \right) \left[ 1 + \sum_{k=0}^{\infty} \frac{\mu'_{2(k+1)}}{k!(k+1)!(2k+1)2^{2k-1}} \right] \right\} d\xi$$

which may be written

$$v_z' = \frac{1}{2\pi} \int_0^c \left( \frac{d\Gamma'}{d\xi} \right) \left\{ \frac{1}{x-\xi} + \frac{x-\xi}{r^2} \left[ \frac{1}{2} + \sum_{k=0}^{\infty} \frac{\mu'_{2(k+1)}}{k!(k+1)!(2k+1)2^{2k}} \right] \right\} d\xi$$

By substituting the numerical values for the coefficients  $\mu'_{2(k+1)}$  from equations (A20) of Appendix A, this equation may be written to an accuracy of three significant figures as

$$v_z' = \frac{1}{2\pi} \int_0^c \left( \frac{d\Gamma'}{d\xi} \right) \left[ \frac{1}{x-\xi} - \frac{0.579}{r^2} (x-\xi) \right] d\xi \quad (20)$$

The foregoing result, which was derived by assuming the fluid to be incompressible, can be modified for the effect of compressibility by the methods of Goldstein and Young. The modification is most readily performed by means of the so-called "Method II" (reference 4, pp. 5-6), which compares the compressible and incompressible flows for equal values of circulation. If the Mach number of the compressible flow at the position of the airfoil is denoted by  $M$ , it is readily shown on the basis of this method that for a given distribution of vorticity the vertical velocity induced in a compressible fluid at any point on the center line of a tunnel of radius  $r$  is  $\sqrt{1-M^2}$  times the corresponding velocity at the same point in an incompressible fluid in a tunnel of radius  $r\sqrt{1-M^2}$ . Thus, from equation (20), the vertical velocity  $v_z'$  in a compressible fluid in the actual tunnel of radius  $r$  is

$$v_z' = \frac{\sqrt{1-M^2}}{2\pi} \int_0^c \left( \frac{d\Gamma'}{d\xi} \right) \left[ \frac{1}{x-\xi} - \frac{0.579}{r^2(1-M^2)} (x-\xi) \right] d\xi \quad (21)$$

The first term of this equation represents the vertical velocity that would be induced by a vortex sheet of infinite span in an unlimited fluid field. The second term thus represents the interference effect of the tunnel wall.

Equation (21) may be compared with the corresponding result from reference 5, which discusses the wall interference for an airfoil in a closed-throat two-dimensional-flow wind tunnel. After alteration to conform with the notation and sign conventions of the present paper, equation (41) of reference 5 gives for the vertical velocity at the camber line of an infinitesimally thin airfoil mounted on the center line of a two-dimensional-flow tunnel of height  $h$

$$v_z' = \frac{\sqrt{1-M^2}}{2\pi} \int_0^c \left( \frac{d\Gamma'}{d\xi} \right) \left[ \frac{1}{x-\xi} - \frac{\pi^2}{6h^2(1-M^2)} (x-\xi) \right] d\xi \quad (22)$$

Comparison of equations (21) and (22) shows that an infinitesimally thin airfoil spanning a closed-throat circular tunnel of radius  $r$  experiences at its midspan section the same interference as would be experienced by the same airfoil in a closed-throat two-dimensional-flow tunnel of height

$$h_1 = \frac{\pi}{\sqrt{6(0.579)}} r = 1.686r$$

or, in terms of the tunnel diameter  $d$ ,

$$h_1 = 0.843d \quad (23)$$

This result makes the later determination of the interference corrections for the circular tunnel very simple, since the corrections for the rectangular tunnel are already known.

It is readily shown by means of equation (6) that the vortex system which represents the infinitesimally thin airfoil induces no axial velocity at any point in the  $xy$ -plane. It follows that airfoil camber has no effect upon the axial velocity or pressure gradient at the position of the model.

**Thickness effect.**—The interference effects associated with airfoil thickness can be found by reducing the given airfoil to its base profile and analyzing the interference between the tunnel wall and this profile. The base profile is defined as the profile the airfoil would have if the camber were removed and the resulting airfoil placed at zero angle of attack. If it is assumed that no wake is present, the interference between the tunnel wall and this symmetrical airfoil can be found by applying the results of equation (5) to Lock's method of analysis of the interference on a symmetrical body in two-dimensional incompressible flow. (Lock's original analysis appears in reference 1; an alternative explanation of the method is given by Glauert in reference 2, pp. 52-57.)

Lock's method of analysis, which assumes that the chord of the airfoil is small as compared with the dimensions of the tunnel, consists essentially in replacing the given symmetrical airfoil by an equivalent two-dimensional source-sink doublet and calculating the interference between this doublet and the tunnel boundaries. The strength of the doublet in any given case is proportioned so that it induces at a considerable distance from itself in free air a velocity equal to the velocity induced at the same point by the original airfoil. In the two-dimensional case, the interference flow at the position of the airfoil is then readily found by introducing an infinite series of images of the doublet such as to satisfy the condition that there shall be no flow normal to the tunnel boundaries and calculating the velocity induced at the airfoil by this system of images. For an airfoil spanning a closed-throat rectangular tunnel at mid-height, the net result of the wall interference for the incompressible case is to increase the effective axial velocity at the position of the airfoil by the amount

$$\Delta_1 V' = \frac{\pi\mu}{6h^2}$$

where  $\mu$  is the strength of the doublet used to represent the airfoil. It is shown in references 4 and 5 that the effect of fluid compressibility is to increase this interference velocity by the factor  $1/[1-(M')^2]^{3/2}$ , where  $M'$  is the Mach number of the undisturbed stream in the tunnel. Thus, in the compressible case,

$$\Delta_1 V' = \frac{\pi\mu}{6h^2[1-(M')^2]^{3/2}} \quad (24)$$

The problem of the symmetrical airfoil in a closed-throat circular tunnel can also be solved by replacing the airfoil by an equivalent doublet spanning the tunnel. In this case, though, the interference for the doublet cannot be found by the method of images. If the doublet used is composed, however, of two vortices in a plane normal to the stream instead of the customary source and sink in line with the stream, the interference velocity can be calculated by means of equation (5). Since the velocity fields of the two types of doublets are identical, the interference calculated by means of the vortex doublet is the same as that which would be obtained if the source-sink doublet were used.

Consider a vortex element of circulation  $\Gamma'$  and span  $d\eta$  at the point  $\omega_0, \theta_0$  in the  $yz$ -plane (fig. 1). From equation (5), the streamwise velocity  $v_x'$  induced at any point  $x, \omega, \theta$  up-

stream from the origin by this element and its accompanying trailing vortices is

$$v_x' = \frac{\partial \phi}{\partial x} = -\frac{\Gamma' d\eta}{\pi r^2} \sum_{m=0}^{\infty} \sum_{s=1}^{\infty} \frac{e^{\lambda_s x} J_m(\lambda_s \omega)}{\left(1 - \frac{m^2}{\lambda_s^2 r^2}\right) \lambda_s J_m^2(\lambda_s r)} \times \left[ m \cos \theta_0 \sin m(\theta - \theta_0) \frac{J_m(\lambda_s \omega_0)}{\omega_0} + \lambda_s \sin \theta_0 \cos m(\theta - \theta_0) J_m'(\lambda_s \omega_0) \right] \quad (25)$$

At a point in the middle plane of the tunnel ( $xy$ -plane),  $\theta = 0$ ,  $\omega = y$ , and the velocity is

$$v_x' = -\frac{\Gamma' d\eta}{\pi r^2} \sum_{m=0}^{\infty} \sum_{s=1}^{\infty} \frac{e^{\lambda_s x} J_m(\lambda_s y)}{\left(1 - \frac{m^2}{\lambda_s^2 r^2}\right) \lambda_s J_m^2(\lambda_s r)} \times \left[ -m \cos \theta_0 \sin m\theta_0 \frac{J_m(\lambda_s \omega_0)}{\omega_0} + \lambda_s \sin \theta_0 \cos m\theta_0 J_m'(\lambda_s \omega_0) \right] \quad (26)$$

As before, the double series in this equation reduces to a single series if the discussion is limited to the interference at the center line of the tunnel. For points on the center line,

$$J_0(\lambda_s y) = J_0(0) = 1$$

$$J_m(\lambda_s y) = J_m(0) = 0 \text{ for } m \geq 1$$

and the streamwise induced velocity becomes

$$v_x' = -\frac{\Gamma' d\eta}{2\pi r^2} \sum_{s=1}^{\infty} \frac{e^{\lambda_s x} \sin \theta_0 J_0'(\lambda_s \omega_0)}{J_0^2(\lambda_s r)} \quad (27)$$

From the known relations for the Bessel functions

$$J_0'(\lambda_s \omega_0) = -J_1(\lambda_s \omega_0) \quad (28)$$

so that equation (27) may be written

$$v_x' = \frac{\Gamma' d\eta}{2\pi r^2} \sum_{s=1}^{\infty} \frac{e^{\lambda_s x} \sin \theta_0 J_1(\lambda_s \omega_0)}{J_0^2(\lambda_s r)} \quad (29)$$

As required by equation (4), the summation with respect to  $s$  in this equation extends over all positive roots of the equation

$$J_0'(\lambda_s r) = -J_1(\lambda_s r) = 0 \quad (30)$$

As the next step, consider a pair of symmetrically placed elementary vortices composed of a vortex of circulation  $-\Gamma'$  at the point  $\omega_0$ ,  $\theta_0$  and a vortex of circulation  $+\Gamma'$  at the point  $\omega_0$ ,  $\theta_0$ . From equation (29), the streamwise velocity induced at a point on the center line of the tunnel by this vortex pair and the accompanying trailing vortices is

$$v_x' = -\frac{\Gamma' d\eta}{\pi r^2} \sum_{s=1}^{\infty} \frac{e^{\lambda_s x} \sin \theta_0 J_1(\lambda_s \omega_0)}{J_0^2(\lambda_s r)} \quad (31)$$

which may also be written

$$v_x' = -\frac{2\Gamma' \omega_0 \sin \theta_0 d\eta}{2\pi r^2 \omega_0} \sum_{s=1}^{\infty} \frac{e^{\lambda_s x} J_1(\lambda_s \omega_0)}{J_0^2(\lambda_s r)} \quad (32)$$

The expression  $(2\Gamma' \omega_0 \sin \theta_0)$  which appears in this equation is the product of the vortex strength and the distance between the vortices.

Now let the distance between the vortices tend to zero while the vortex strength increases in such a way that the product  $(2\Gamma' \omega_0 \sin \theta_0)$  retains a constant value  $\mu$ . The result in the limit is an elementary vortex doublet of strength  $\mu$  and span  $d\eta$  at the point  $\omega_0 = \eta$  on the  $y$ -axis. The streamwise velocity induced on the center line of the tunnel by this elementary spanwise doublet and the accompanying trailing vortex doublets is then

$$v_x' = -\frac{\mu d\eta}{2\pi r^2} \sum_{s=1}^{\infty} \frac{e^{\lambda_s x} J_1(\lambda_s \eta)}{J_0^2(\lambda_s r)} \quad (33)$$

As before, the infinite series in this equation is rapidly convergent for large negative values of  $x$ , but the convergence is slow for small negative values and is nonexistent when  $x = 0$ . Once again, however, the series can be expressed as a combination of elementary functions and a power series which is readily applied to the problem at hand. The details of the transformation are given in Appendix A. By means of the final result, equation (33) can be written

$$v_x' = -\frac{\mu d\eta}{2\pi r^2} \left[ \frac{r^2}{2(\eta^2 + x^2)^{3/2}} - \sum_{k=0}^{\infty} \sum_{p=0}^{\infty} \frac{(-1)^p \mu_2(k+p+1) \eta^{2k} x^{2p}}{k!(k+1)!(2p)!(2k+1)r^{2k+2p+1}} \right] \quad (34)$$

where the double summation extends over all integral values of  $k$  and  $p$  from zero to infinity. The coefficient  $\mu_2(k+p+1) = \mu_{2f}$  is given by the integral

$$\mu_{2f} = \frac{1}{(2f+1)\pi} \int_0^{\infty} \frac{t^{2f} dt}{I_1^2(t)} \quad (35)$$

The numerical values of this integral for  $f = 1, 2, 3, 4$  are evaluated in Appendix A.

The induced velocity for a doublet spanning the tunnel is now readily found by taking the doublet strength  $\mu$  constant across the span and integrating equation (34) with respect to  $\eta$  from  $-r$  to  $+r$ . This gives finally

$$v_x' = -\frac{\mu}{2\pi r^2} \left[ \frac{r^3}{x^2 \sqrt{r^2 + x^2}} - \sum_{k=0}^{\infty} \sum_{p=0}^{\infty} \frac{(-1)^p \mu_2(k+p+1) x^{2p}}{k!(k+1)!(2p)!(2k+1)2^{2k+2p}} \right] \quad (36)$$

In the integration across the tunnel, all the trailing vortices, of course, disappear.

It is apparent from the symmetry of the problem, that the streamwise velocity induced by a doublet spanning the tunnel must be an even function of the variable  $x$ . Equation (36), which was derived for negative values of  $x$ , is seen to be such a function and is thus applicable to positive values of the variable as well.

The values of  $v_x'$  for vanishingly small values of  $x$ , that is, at the position of the doublet, is then found from equation (36) by expanding the first term in ascending powers of  $x/r$  and discarding all terms containing second powers and higher and by retaining only the  $p = 0$  terms of the double series. This gives

$$v_x' = -\frac{\mu}{2\pi r^2} \left[ \frac{r^2}{x^2} - \frac{1}{2} - \sum_{k=0}^{\infty} \frac{\mu_2(k+1)}{k!(k+1)!(2k+1)2^{2k}} \right] \quad (37)$$

After substitution of the numerical values for the coefficients  $\mu_{2(k+1)}$  from equations (A33) of Appendix A, this equation becomes to an accuracy of three significant figures

$$v_z' = -\frac{\mu}{2\pi x^2} + \frac{1.356\mu}{2\pi r^2} \quad (38)$$

The first term of equation (38) is the velocity induced by a doublet of infinite span in a field of unlimited extent. The remaining term therefore represents the effect of interference between the doublet and the tunnel wall. Thus the net result of the interference between the airfoil thickness and the tunnel wall for the incompressible fluid is to increase the effective stream velocity at the position of the airfoil by the amount

$$\Delta_1 V' = \frac{1.356\mu}{2\pi r^2} \quad (39)$$

In any particular case,  $\mu$  is again equal to the strength of the doublet used to represent the given airfoil.

The result of equation (39) can be modified for the effect of fluid compressibility by the method of reference 4. In this case, the modification is most conveniently performed by means of Method I (reference 4, pp. 3-5) which compares the compressible and incompressible flows for a given airfoil of unaltered shape and size. By this method, it is readily shown that the streamwise velocity induced in the incompressible fluid at any point on the center line of a tunnel of radius  $r$  is  $1/\sqrt{1-(M')^2}$  times the corresponding velocity at the same point in an incompressible fluid in a tunnel of radius  $r\sqrt{1-(M')^2}$ . Here  $M'$  is, as before, the Mach number in the undisturbed stream. The increment in axial velocity in the compressible case is thus

$$\Delta_1 V' = \frac{1.356\mu}{2\pi r^2 [1-(M')^2]^{3/2}} \quad (40)$$

Comparison of equations (24) and (40) shows that, if no wake is present, a symmetrical airfoil spanning a closed-throat circular tunnel of radius  $r$  experiences at its midspan section the same increase in axial velocity as would be experienced by the same airfoil in a closed-throat two-dimensional-flow tunnel of height

$$h_2 = \frac{\pi}{\sqrt{3}(1.356)} r = 1.558r$$

or, in terms of the tunnel diameter,

$$h_2 = 0.779d \quad (41)$$

The foregoing result greatly simplifies the determination of the true stream conditions at the position of the airfoil in the circular tunnel, since the necessary equations for the rectangular tunnel are already known.

Consideration of the symmetry of the system formed by a base profile spanning the middle of a circular tunnel indicates that the interference between the wall and the airfoil thickness does not influence the vertical induced velocity  $v_z'$  at any point on the airfoil. Similarly, the airfoil thickness has no effect upon the streamwise pressure gradient in the tunnel at the position of the airfoil.

**Wake effect.**—It is shown in general terms in reference 5 that the interference between the wake of a body and the walls of a closed-throat wind tunnel gives rise at the position of the body to a velocity increment and a streamwise pressure gradient which are not present in free air. This is true for any type of body and any shape of tunnel test section. The magnitude of this velocity increment and pressure gradient in the case of an airfoil spanning a closed-throat rectangular tunnel can be determined approximately by replacing the wake by the flow from a suitable fluid source and the tunnel walls by an infinite system of image sources. In the case of the airfoil spanning a closed-throat circular tunnel, this treatment is no longer possible, since no system of image sources is known which will satisfy the boundary conditions at the tunnel wall. A more complex method of analysis could conceivably be devised for this case; however, since the calculation is highly approximate even in the case of two-dimensional flow, such an analysis does not appear warranted. For present purposes it is probably sufficient to assume that the midspan section of the airfoil in the circular tunnel experiences the same velocity increment and pressure gradient as a result of the wake interference as does the same airfoil in a rectangular tunnel of a height defined by equation (41). This assumption leads to the simplest expression for the final correction to the measured drag coefficient and should give results which are reasonably accurate. If it is assumed that the center of the wake lies in a horizontal plane containing the diameter of the tunnel, it follows from considerations of symmetry that the wake interference does not contribute to the vertical induced velocity  $v_z'$  at the airfoil.

It has already been indicated that the interference associated with the camber of the airfoil has no effect upon the stream velocity at the model. The total increase in velocity for the complete airfoil in the circular tunnel is thus given by the sum of the increments caused by the thickness and the wake of the airfoil. In reference 5 it is shown that for the analogous case of the airfoil in the rectangular tunnel, the true velocity  $V$  at the position of the airfoil may finally be written

$$V = V' \left\{ 1 + \frac{1}{[1-(M')^2]^{3/2}} \Delta\sigma + \frac{1+0.4(M')^2}{1-(M')^2} \tau c_a' \right\} \quad (42)$$

where  $\sigma$  and  $\tau$  are factors dependent upon the size of the airfoil relative to the tunnel,  $\Delta$  is a factor dependent upon the shape of the base profile, and  $c_a'$  is the drag coefficient of the airfoil as measured in the tunnel. The first correction term in this equation represents the velocity increment caused by the airfoil thickness and is found by substituting the proper value for the equivalent doublet strength in equation (24). The second correction term represents the velocity increment associated with the wake of the airfoil.

The factors  $\sigma$  and  $\tau$  in equation (42) are defined by

$$\sigma = \frac{\pi^2}{48} \left( \frac{c}{h} \right)^2 \quad (43)$$

and

$$\tau = \frac{1}{4} \left( \frac{c}{h} \right) \quad (44)$$

where  $(c/h)$  is the ratio of the airfoil chord to the tunnel height. An analytic expression for  $\Lambda$  is given in equation (3) of reference 5. Values of  $\Lambda$  for a number of base profiles are given in table I, which is reproduced from this reference.

If it is assumed that the height of the equivalent rectangular tunnel with regard to the wake interference is the same as that given by equation (41) for the thickness interference, the true velocity in the circular tunnel is found simply by substituting  $h_2$  from equation (41) for  $h$  in the factors  $\sigma$  and  $\tau$  of equation (42). The true velocity at the midspan section of an airfoil spanning a circular tunnel is thus

$$V = V' \left\{ 1 + \frac{1}{[1 - (M')^2]^{3/2}} \Lambda \sigma_2 + \frac{1 + 0.4(M')^2}{1 - (M')^2} \tau_2 c_d' \right\} \quad (45)$$

where the factors  $\tau_2$  and  $\sigma_2$  are defined by

$$\tau_2 = 0.321 \left( \frac{c}{d} \right) \quad (46)$$

and

$$\sigma_2 = 0.339 \left( \frac{c}{d} \right)^2 \quad (47)$$

A correction to the stream velocity implies corrections also to the stream dynamic pressure, Reynolds number and Mach number. These corrections for an airfoil spanning a rectangular tunnel have been determined in reference 5 on the basis of the assumption that the flow is adiabatic. The corresponding corrections for the circular tunnel can be found by replacing the factors  $\tau$  and  $\sigma$  in equations (29), (32), and (33) of reference 5 by the factors  $\tau_2$  and  $\sigma_2$  of the present paper. The true dynamic pressure  $q$ , Reynolds number  $R$ , and Mach number  $M$  at the midspan section in the circular tunnel are thus related to the corresponding quantities in the undisturbed stream (denoted by primes) by the equations

$$q = q' \left\{ 1 + \frac{2 - (M')^2}{[1 - (M')^2]^{3/2}} \Lambda \sigma_2 + \frac{[2 - (M')^2][1 + 0.4(M')^2]}{1 - (M')^2} \tau_2 c_d' \right\} \quad (48)$$

$$R = R' \left\{ 1 + \frac{1 - 0.7(M')^2}{[1 - (M')^2]^{3/2}} \Lambda \sigma_2 + \frac{[1 - 0.7(M')^2][1 + 0.4(M')^2]}{1 - (M')^2} \tau_2 c_d' \right\} \quad (49)$$

$$M = M' \left\{ 1 + \frac{1 + 0.2(M')^2}{[1 - (M')^2]^{3/2}} \Lambda \sigma_2 + \frac{[1 + 0.2(M')^2][1 + 0.4(M')^2]}{1 - (M')^2} \tau_2 c_d' \right\} \quad (50)$$

Numerical values of the functions of  $M'$  which appear in these equations are given in table II, which is reproduced from reference 5.

At low Mach numbers, the terms containing  $\tau_2 c_d'$  in the equations for the corrected stream characteristics are usually negligible as compared with the terms containing  $\Lambda \sigma_2$ . At high Mach numbers, however, where the drag coefficient is very large, the terms with  $\tau_2 c_d'$  predominate.

#### RELATIONS BETWEEN AIRFOIL CHARACTERISTICS IN TUNNEL AND IN FREE AIR

The characteristics of the airfoil in free air are now readily determined in terms of the characteristics at the midspan

section in the tunnel. It is simply necessary to apply the results of the preceding sections to the relations already derived in reference 5 for the airfoil spanning a rectangular tunnel.

Briefly, the method of reference 5 relates the section characteristics in the tunnel at an undisturbed stream velocity  $V'$  to the characteristics in an unconfined stream having a velocity equal to the true velocity  $V$  which exists at the position of the airfoil in the tunnel. The relation is obtained on the basis of equal values of the so-called cotangent component of lift in the tunnel and in free air, this being necessary to assure that the essential character of the pressure distribution over the airfoil is the same in both cases. By this procedure corrections are derived which may be applied to simultaneously measured lift, moment, and drag coefficients and angle of attack in the tunnel to obtain the corresponding quantities in free air. These corrections appear as functions of the factors  $\Lambda$  and  $\sigma$ , of the product  $\tau c_d'$ , and of the Mach number  $M'$  of the undisturbed stream. The correction to the angle of attack, which arises out of the interference effects associated with camber, is proportional to  $\sigma$  and independent of  $\Lambda$  and  $\tau c_d'$ . The correction equations for the lift and moment coefficients contain corresponding terms proportional to  $\sigma$  alone, together with terms which depend upon the thickness and the wake effects and are proportional to the products  $\Lambda \sigma$  and  $\tau c_d'$ . The correction to the drag coefficient appears as two terms, proportional to  $\Lambda \sigma$  and  $\tau c_d'$ , respectively. The term proportional to  $\Lambda \sigma$  in this case composed basically of two parts, one due to the thickness effect and one due to the wake effect.

The correction equations for the airfoil spanning a circular tunnel can be derived directly by modifying the equations of reference 5 in accordance with the results of the preceding sections. Since the terms containing  $\sigma$  exclusive of  $\Lambda$  appear as a result of the camber effect, the tunnel height  $h$  in such terms must be replaced by  $0.843d$  as required by equation (23). In the terms which depend upon the thickness and wake effects and are distinguished by the products  $\Lambda \sigma$  and  $\tau c_d'$ , the quantity  $h$  is replaced by  $0.779d$  in accordance with equation (41). This involves the assumption already mentioned that the height of the equivalent rectangular tunnel with regard to the wake effect is the same as that calculated for the thickness effect.

As in reference 5, the free-air lift, quarter-chord-moment, and drag coefficients referred to the true dynamic pressure  $q$  are denoted by the conventional symbols. The corresponding quantities measured in the tunnel and referred to the apparent dynamic pressure  $q'$  are denoted by the same symbols with primes added. The final equations for the corrected aerodynamic coefficients are then

$$c_i = c_i' \left\{ 1 - \frac{\sigma_1}{1 - (M')^2} - \frac{2 - (M')^2}{[1 - (M')^2]^{3/2}} \Lambda \sigma_2 - \frac{[2 - (M')^2][1 + 0.4(M')^2]}{1 - (M')^2} \tau_2 c_d' \right\} \quad (51)$$

$$c_{m_{c/4}} = c_{m_{c/4}}' \left\{ 1 - \frac{2 - (M')^2}{[1 - (M')^2]^{3/2}} \Lambda \sigma_2 - \frac{[2 - (M')^2][1 + 0.4(M')^2]}{1 - (M')^2} \tau_2 c_d' \right\} + c_i' \frac{\sigma}{4[1 - (M')^2]} \quad (52)$$

$$c_d = c_d' \left\{ 1 - \frac{3 - 0.6(M')^2}{[1 - (M')^2]^{3/2}} \Delta\sigma_2 - \frac{[2 - (M')^2][1 + 0.4(M')^2]}{1 - (M')^2} \tau_2 c_d' \right\} \quad (53)$$

and the corresponding angle of attack in degrees is

$$\alpha = \alpha' + \frac{57.3\sigma_1}{2\pi\sqrt{1 - (M')^2}} \left\{ c_i' + 4c_{m_c/h}' \right\} \quad (54)$$

where the factor  $\sigma_1$  is given by

$$\sigma_1 = 0.289 \left( \frac{c}{d} \right)^2 \quad (55)$$

and the factors  $\tau_2$  and  $\sigma_2$  are as already defined in equations (46) and (47). Numerical values of the compressibility factors which appear in these equations are given in table II. The corrected quantities correspond to the true Reynolds number and true Mach number as given by equations (49) and (50).

From a rigorous standpoint, the foregoing corrections apply only to data obtained from chordwise pressure distributions at the midspan section of the airfoil. Actually, as has already been pointed out in the discussion of camber effect, the experimental chordwise pressure distribution at any given angle of attack is sensibly constant across the span. The corrections should therefore be applicable with sufficient accuracy to data obtained from pressure distributions at any spanwise station.

Reference 5 also includes a method for correcting experimental chordwise pressure distributions to free-air conditions in the case of an airfoil spanning a rectangular tunnel. The same procedure may be applied to pressure distributions over an airfoil spanning a circular tunnel if the factor  $\tau$  is replaced by  $\tau_2$  and the factor  $\sigma$  by  $\sigma_1$  wherever it appears alone and by  $\sigma_2$  where it appears in the product  $\Delta\sigma$ .

CHOKING AT HIGH SPEEDS

As explained in reference 5, for tests of a model in any closed-throat wind tunnel, there is some value of the Mach number  $M'$  of the undisturbed stream which cannot be exceeded irrespective of the power input to the tunnel. This follows from the fact that at high speeds the combination of model and wind tunnel acts essentially as a converging-diverging nozzle, and the flow in the tunnel exhibits the characteristics of the flow in such a nozzle. Thus, at some Mach number less than unity in the undisturbed stream, sonic velocity is attained at all points across a section of the tunnel, usually in the vicinity of the model. When this occurs, increased power input to the tunnel serves merely to extend the region of supersonic flow downstream of this sonic section and has no effect upon the velocity of the stream ahead of the model. The tunnel is then said to be "choked", and the Mach number  $M'$  of the undisturbed flow ahead of the airfoil has its maximum attainable value. This value is described as the apparent choking Mach number, the word "apparent" being used to differentiate this value from the corresponding free-air Mach number  $M$  which would be computed from equation (50).

If it is assumed that the section of sonic velocity is coincident with the section of minimum area between the model and the tunnel walls, the apparent choking Mach number can be obtained from elementary considerations of uni-dimensional adiabatic flow, as shown in reference 5. For the present case of a constant-chord airfoil spanning a circular tunnel, the apparent choking Mach number  $M'_{ch}$  is finally defined for air ( $\gamma=1.4$ ) by the relation

$$\frac{4}{\pi} \left( \frac{t_e}{d} \right) = 1 - \left[ 1 + \frac{(M'_{ch})^2 - 1}{6} \right]^3 \quad (56)$$

where  $t_e$  is the "effective" thickness of the airfoil and  $d$  is, as before, the diameter of the tunnel. A graph of this relation is given in figure 4. As a matter of interest, the results are shown for the supersonic as well as the subsonic flow regime. The region above the curve represents an impossible state of flow.

In estimating the apparent choking Mach number in any practical case it is necessary to replace the effective thickness  $t_e$  by the projected thickness  $t_p$  of the airfoil normal to the direction of flow. As indicated in reference 5, this procedure leads, in the case of the subsonic wind tunnel, to an over-estimation of  $M'_{ch}$  because it neglects the possible contraction of a portion of the stream aft of the airfoil as well as the effect of the airfoil boundary layer.

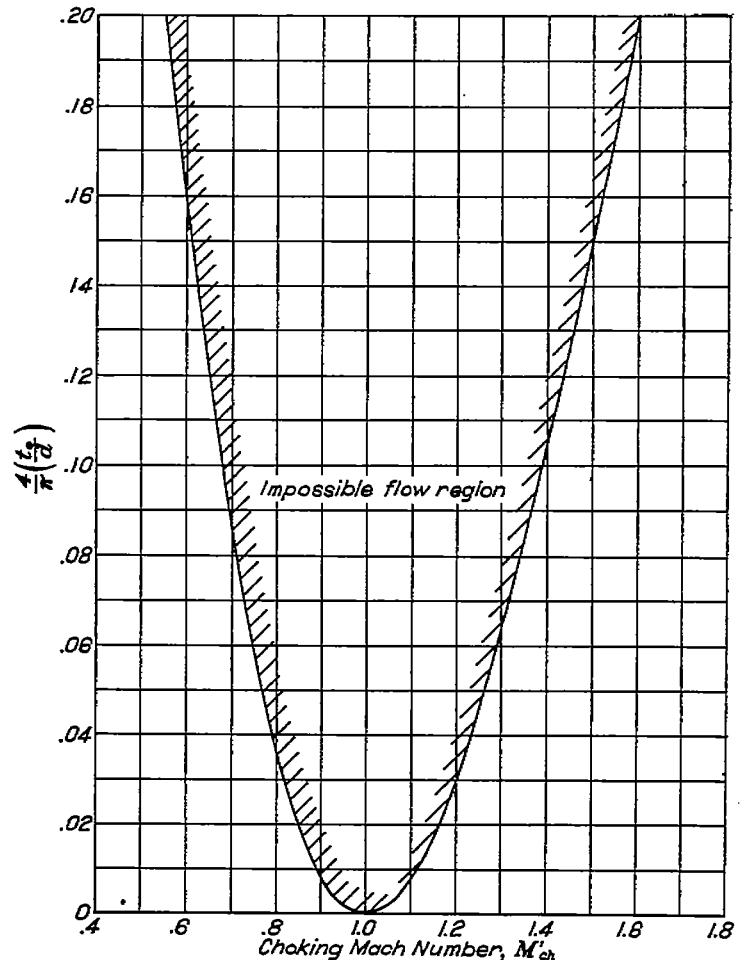


FIGURE 4.—Choking Mach number as determined by airfoil thickness.

The importance of the boundary layer and the accompanying drag with regard to tunnel choking is pointed out in reference 5, where the apparent choking Mach number is calculated for a flat plate at zero angle of attack in a two-dimensional-flow wind tunnel. Since the projected thickness for the plate is zero, the unidimensional theory would indicate that no choking occurs. Actually, because of the fact that the plate experiences drag, choking does take place. Similar considerations hold, of course, for a flat plate spanning a circular tunnel. In this case the apparent choking Mach number for air ( $\gamma=1.4$ ) is given by the equation

$$\frac{1}{\pi} \left( \frac{c}{d} \right) c_d' = \frac{1+1.4(M'_{ch})^2}{2.8(M'_{ch})^2} \left\{ 1 - \sqrt{1 - \left[ \frac{1-(M'_{ch})^2}{1+1.4(M'_{ch})^2} \right]^2} \right\} \quad (57)$$

A graph of this relation is given in figure 5. The effect of drag on choking for supersonic as well as subsonic wind tunnels is shown. It can be demonstrated that the points on the curve correspond to a Mach number of unity in the flow far downstream of the model where the wake has spread completely to the tunnel wall. Points above the curve represent impossible conditions of flow. In most cases encountered in subsonic tunnels, the apparent choking Mach number determined by the thickness of the airfoil and defined by equation (56) is usually the lower. For very thin airfoils at small angles of attack, however, the value of  $M'_{ch}$  given by equation (57) can have the lower value. At present

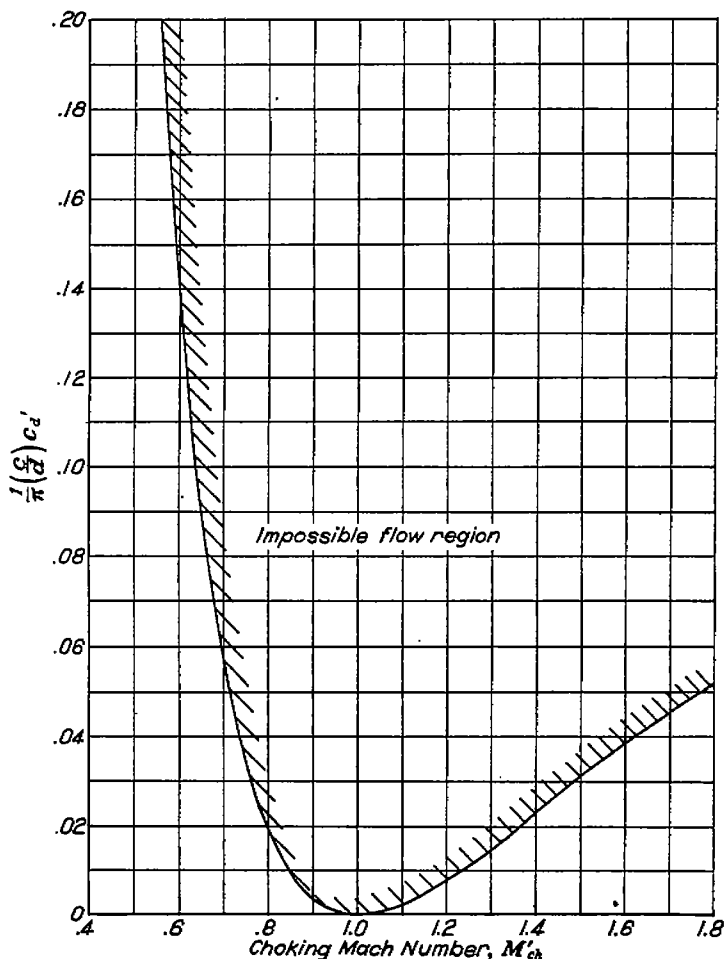


FIGURE 5.—Choking Mach number as determined by airfoil drag.

no way is known to combine the thickness and drag effects in a single calculation as should logically be done.

It should be noted, as pointed out in detail in reference 5, that the flow in a tunnel at choking does not correspond to any flow in free air. Furthermore, for a range of Mach numbers just below choking, where the flow is influenced to any extent by the restrictions which finally promote choking, any wall-interference correction is of doubtful accuracy. This is particularly true if the model is at an appreciable angle of attack so that sonic velocity is attained across the stream on one side of the airfoil before it is on the other.

#### EXPERIMENT

The experimental investigation was initiated for two reasons: (1) to determine the spanwise distribution of lift over an airfoil spanning a closed-throat circular tunnel, and (2) to examine the validity of the theoretical interference corrections derived in the preceding analysis. As has been previously mentioned, the development of the theoretical relations requires a knowledge of the variation in lift over the span of the airfoil. Since no theoretical or experimental evidence regarding this matter was available, the spanwise variation in lift was investigated experimentally for an NACA 4412 airfoil for two ratios of airfoil chord to tunnel diameter. The results of these tests are also directly applicable to the examination of the validity of the theoretical correction equations.

The experimental work was performed in a low-turbulence, nonreturn-type wind tunnel with interchangeable throat sections of 14- and 8-inch diameter. The two chord-diameter ratios were obtained by testing the same airfoil in each throat section. Since the airspeed was held constant throughout the tests, this arrangement permitted the Reynolds number and the Mach number to be duplicated simultaneously for the two chord-diameter ratios. In this manner the effects of any variation in these parameters were eliminated from the tests.

The NACA 4412 airfoil was used because a model of suitable size was already available ideally equipped for pressure-distribution tests. The model, which is described in reference 16, was of 5-inch chord and 30-inch span. This chord, together with the two throat diameters, gave chord-diameter ratios of 0.357 and 0.625. In the tests, the airfoil extended through the walls of the tunnel and was clamped in tight-fitting support blocks which prevented any leakage of air at the walls. The 54 pressure orifices located around the surface of the midspan section of the model were connected to a multiple-tube manometer for measurement of the pressure distribution over the airfoil. To secure as accurate pressure-distribution data as possible, alcohol was used as the manometer fluid and the liquid heights were recorded photographically.

Pressure-distribution records were secured at each of eight angles of attack from  $-4^\circ$  to  $15^\circ$  at a Reynolds number of approximately 450,000 and a Mach number of approximately 0.2 with the model mounted in both the 14-inch and the 8-inch diameter throats. The spanwise distribution of lift was determined for each angle of attack by sliding the pressure orifices laterally from one wall to the other and recording the

indicated pressure distributions at a number of spanwise stations. The chordwise pressure distributions were plotted and mechanically integrated to obtain lift and quarter-chord moment coefficients. No drag coefficients were obtained because the experimental installation did not permit balance measurements to be made and wake surveys were not feasible.

By testing the airfoil in both erect and inverted attitudes the inclination of the air stream with respect to the tunnel axis was determined for each throat section. The stream angle was found to be  $+0.45^\circ$  for the 14-inch throat and  $0^\circ$  for the 8-inch throat. Corrections have been applied to all angles of attack for the measured angularity.

The spanwise distribution of lift coefficient uncorrected for tunnel-wall interference is shown for the two chord-diameter ratios in figures 6 and 7 in which lift coefficients at various angles of attack are plotted as a function of the spanwise location of the measurement plane.

Curves of lift coefficient against angle of attack for the two chord-diameter ratios are shown uncorrected for tunnel-wall interference in figure 8 (a). The results given pertain to the section of the airfoil at the center line of the tunnel. The corresponding curves corrected for wall interference by means of equations (51) and (54) are shown in figure 8 (b). In applying the corrections, the term containing  $\tau c_d'$  was necessarily omitted as no measurements of drag were made. For the values of  $c_d$  to be expected in such tests, however,

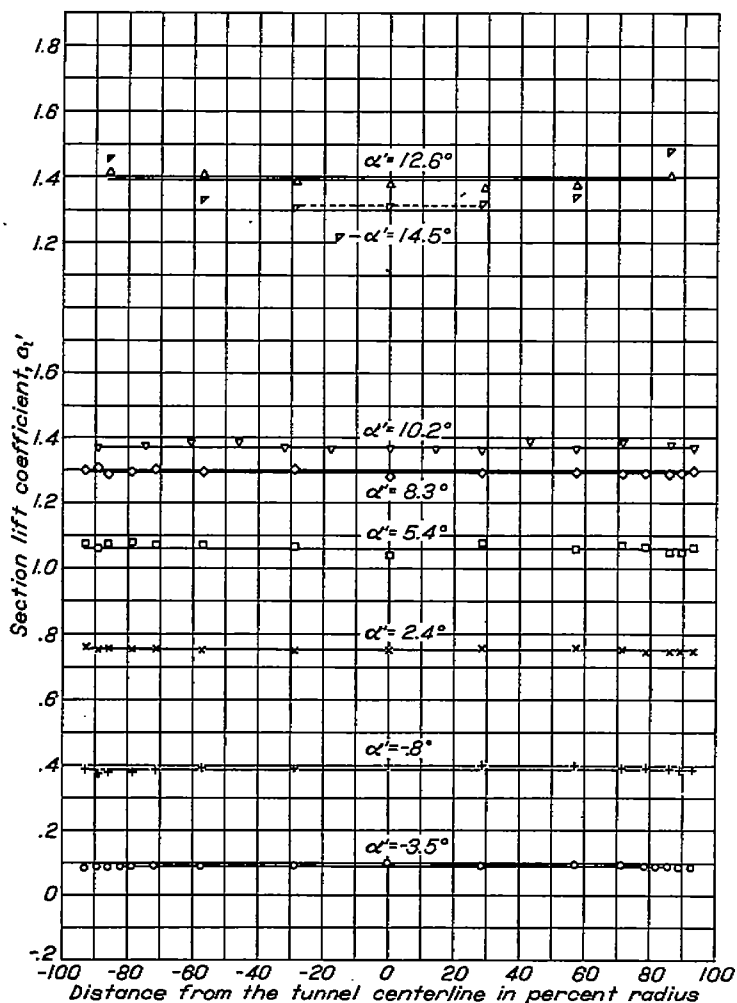


FIGURE 6.—Spanwise lift distribution for the NACA 4412 airfoil.  $c/d = .357$ .

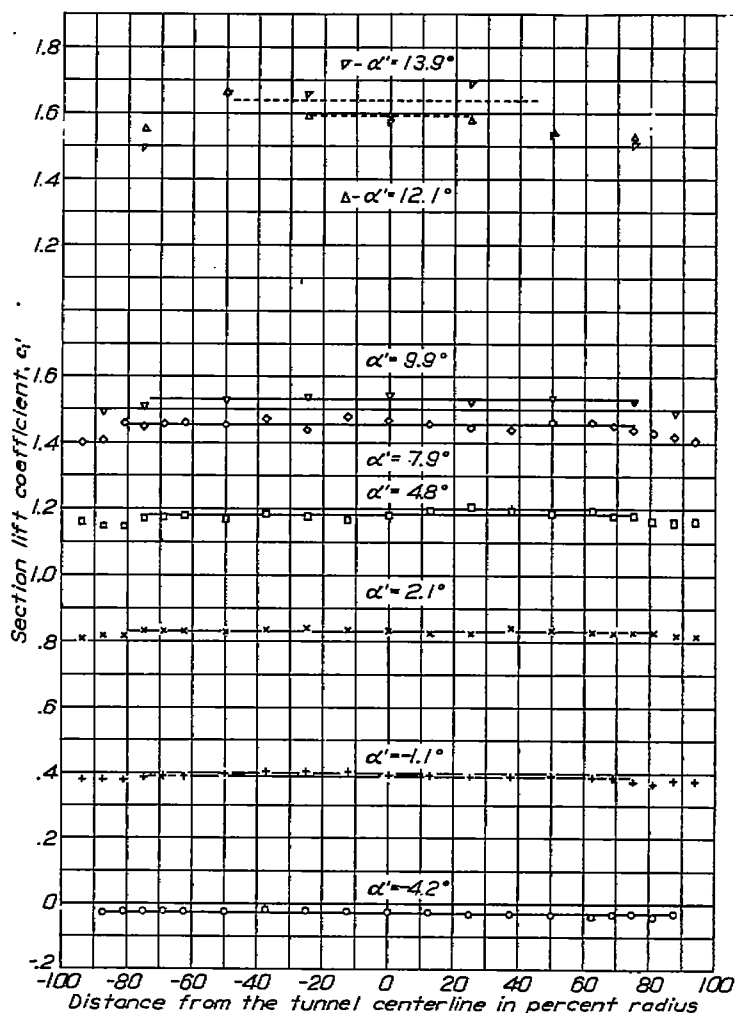


FIGURE 7.—Spanwise lift distribution for the NACA 4412 airfoil.  $c/d = .625$ .

this term would be negligible in comparison with the remaining terms so that this omission does not affect the final results. For purposes of comparison, section lift characteristics as obtained by Pinkerton from tests of a finite-span rectangular airfoil in the Langley variable-density wind tunnel (reference 17) are also shown. These data correspond to an effective Reynolds number of 450,000 and are thus directly comparable to the results of the present test.

In figure 9 (a) curves of quarter-chord moment coefficient against lift coefficient are shown uncorrected for tunnel-wall interference for both chord-diameter ratios. The same data are plotted in figure 9 (b) after correction for wall interference by means of equations (51) and (52). Also shown for comparison are the corresponding data from reference 17.

### DISCUSSION

An examination of figures 6 and 7 reveals the previously mentioned fact that there is no appreciable variation in lift over the span of the airfoil at all angles of attack up to those closely approaching the stalling angle. This observation holds for both chord-diameter ratios. In the vicinity of the stall a spanwise variation in lift appears which becomes progressively more erratic as the angle of attack is increased. As might be expected, this variation becomes apparent at a lower angle in the case of the larger chord-diameter ratio. The results of figures 6 and 7 corroborate the conclusion of

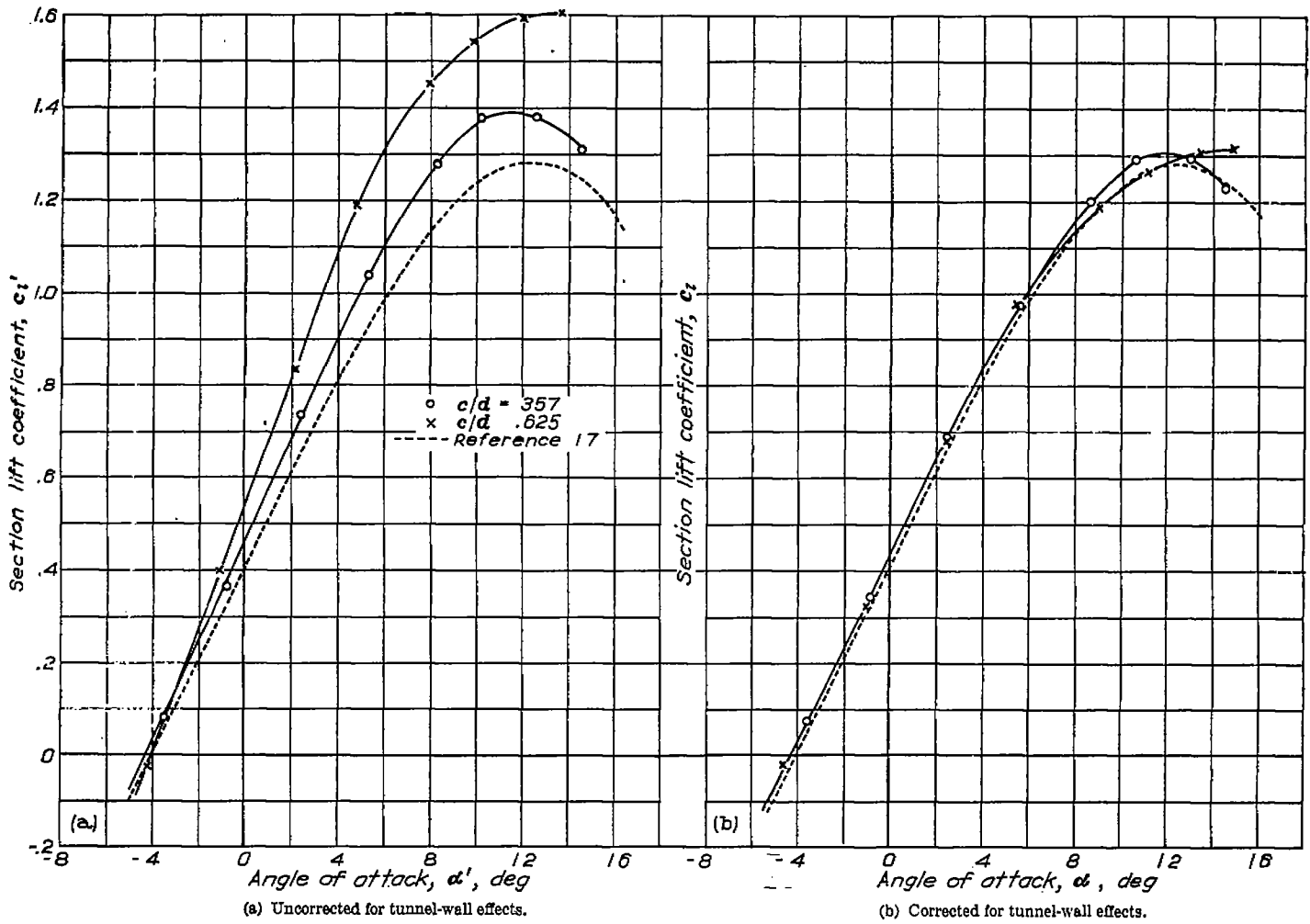


FIGURE 8.—Variation of section lift coefficient with angle of attack for the NACA 4412 airfoil.

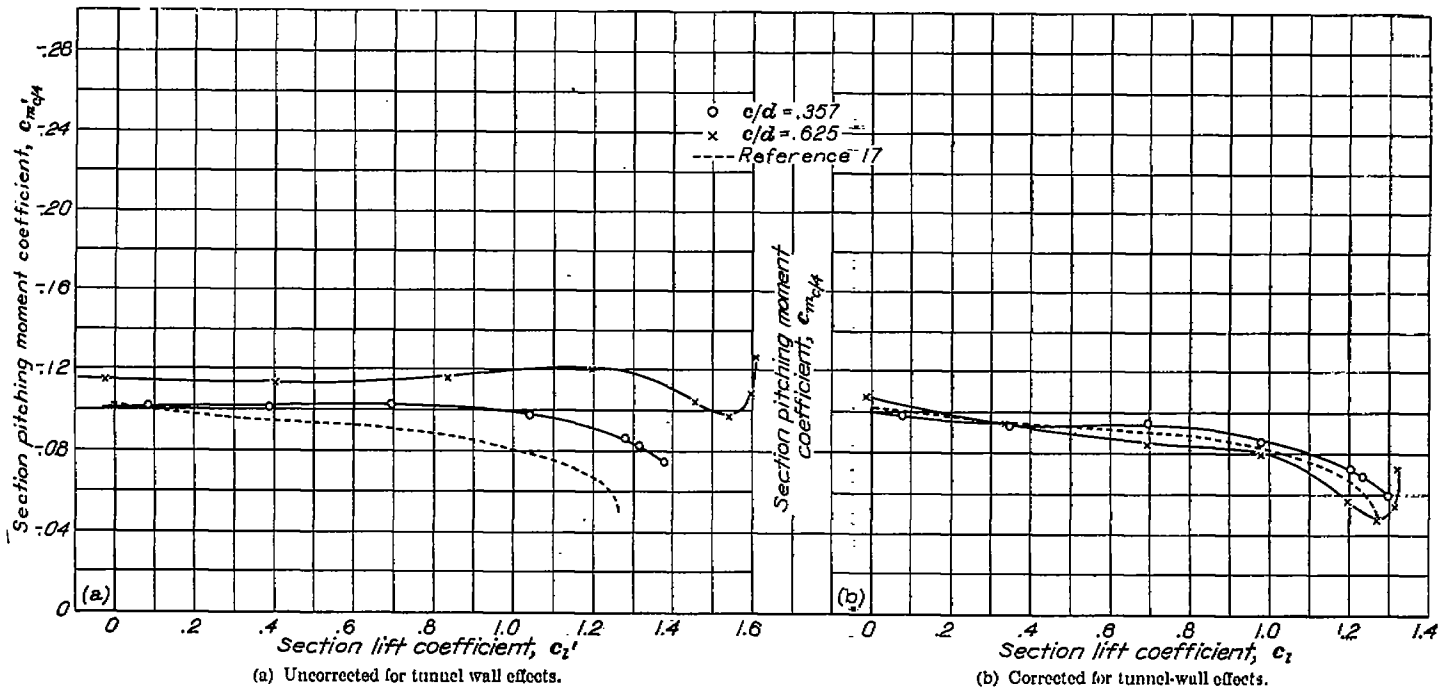


FIGURE 9.—Variation of section pitching moment coefficient with section lift coefficient for the NACA 4412 airfoil.

Appendix B for the particular case of the airfoil spanning a circular tunnel.

From figure 8 (b), it is seen that the corrected lift curves for the two chord-diameter ratios agree almost exactly with one another except at angles near the stall. Below the vicinity of the stall the corrected data coincide with the results of reference 17 except for a constant angular displacement of approximately  $0.2^\circ$ . In reference 16, Pinkerton estimates that his values for the angles of attack may be too large by a constant error of approximately  $0.25^\circ$  because of a possible error in the assumed direction of the stream. It is thought that the angles of attack of the present experiments are accurate to within  $\pm 0.1^\circ$ . These limits of accuracy are sufficient to account completely for the apparent angular displacement.

In the region of the stall, the corrected lift curves for the two chord-diameter ratios do not mutually coincide, but the data for the chord-diameter ratio of 0.357 agree with Pinkerton's results within 2 percent. As previously mentioned, Pinkerton's tests were made with a finite-span rectangular airfoil, for which the cross-span variation in lift is necessarily large. It is not to be expected that the determination of maximum section lift from such tests would be as accurate as from tests of a through model, for which the cross-span lift variation is small.

It is seen from figure 9(b) that the corrected moment curves agree satisfactorily with each other and with the results of reference 17.

In summary, for angles of attack below those in the region of maximum lift, the results presented in figures 8 and 9 demonstrate the validity of the theoretical lift, moment, and angle-of-attack corrections for low Mach numbers and chord-diameter ratios up to at least 0.625. For angles in the vicinity of maximum lift, the corrections are not strictly applicable up to such a large chord-diameter ratio. The results of the present test indicate that an accurate determination of maximum lift can be made with a chord-diameter ratio at least as high as 0.35. An evaluation of the accuracy of the correction equations at high Mach numbers is not possible on the basis of the experimental evidence available at present. It is to be expected, however, that the maximum permissible chord-diameter ratios will decrease as the Mach number increases.

The data of the present paper enable no definite conclusions to be drawn regarding the validity of the drag correction. However, in view of the accuracy of the other corrections for the circular tunnel and in view of the fact that the corresponding drag correction for a two-dimensional tunnel is known to be accurate, it is to be expected that this correction will give a satisfactory evaluation of the wall interference upon the measured drag.

The equations of the present paper should not be expected to give accurate results when applied to tests in which air leakage occurs at the tunnel walls. In such tests the lift at the walls drops markedly, so that the assumption that the lift is uniform across the span is no longer valid. The importance of avoiding such leakage, if reliable airfoil characteristics are to be obtained, is pointed out in reference

5 with regard to tests in two-dimensional tunnels. The same general considerations apply in the case of an airfoil spanning a circular tunnel.

### CONCLUSIONS

Airfoil data obtained from tests at subsonic speeds of an airfoil spanning the center of a closed-throat circular wind tunnel can be corrected to free-air conditions by means of the following equations:

$$V = V' \left\{ 1 + \frac{1}{[1 - (M')^2]^{3/2}} \Delta\sigma_2 + \frac{1 + 0.4(M')^2}{1 - (M')^2} \tau_2 c_d' \right\} \quad (45)$$

$$q = q' \left\{ 1 + \frac{2 - (M')^2}{[1 - (M')^2]^{3/2}} \Delta\sigma_2 + \frac{[2 - (M')^2][1 + 0.4(M')^2]}{1 - (M')^2} \tau_2 c_d' \right\} \quad (48)$$

$$R = R' \left\{ 1 + \frac{1 - 0.7(M')^2}{[1 - (M')^2]^{3/2}} \Delta\sigma_2 + \frac{[1 - 0.7(M')^2][1 + 0.4(M')^2]}{1 - (M')^2} \tau_2 c_d' \right\} \quad (49)$$

$$M = M' \left\{ 1 + \frac{1 + 0.2(M')^2}{[1 - (M')^2]^{3/2}} \Delta\sigma_2 + \frac{[1 + 0.2(M')^2][1 + 0.4(M')^2]}{1 - (M')^2} \tau_2 c_d' \right\} \quad (50)$$

$$\alpha = \alpha' + \frac{57.3\sigma_1}{2\pi\sqrt{1 - (M')^2}} \left\{ c_i' + 4c_{m_{c_d'}} \right\} \text{ (deg)} \quad (54)$$

$$c_i = c_i' \left\{ 1 - \frac{\sigma_1}{1 - (M')^2} - \frac{2 - (M')^2}{[1 - (M')^2]^{3/2}} \Delta\sigma_2 - \frac{[2 - (M')^2][1 + 0.4(M')^2]}{1 - (M')^2} \tau_2 c_d' \right\} \quad (51)$$

$$c_{m_{c_d}} = c_{m_{c_d}}' \left\{ 1 - \frac{2 - (M')^2}{[1 - (M')^2]^{3/2}} \Delta\sigma_2 - \frac{[2 - (M')^2][1 + 0.4(M')^2]}{1 - (M')^2} \tau_2 c_d' \right\} + c_i' \frac{\sigma_1}{4[1 - (M')^2]} \quad (52)$$

$$c_d = c_d' \left\{ 1 - \frac{3 - 0.6(M')^2}{[1 - (M')^2]^{3/2}} \Delta\sigma_2 - \frac{[2 - (M')^2][1 + 0.4(M')^2]}{1 - (M')^2} \tau_2 c_d' \right\} \quad (53)$$

where  $\tau_2$ ,  $\sigma_1$ , and  $\sigma_2$  are given by

$$\tau_2 = 0.321 \left( \frac{c}{d} \right) \quad (46)$$

$$\sigma_1 = 0.289 \left( \frac{c}{d} \right)^2 \quad (55)$$

$$\sigma_2 = 0.339 \left( \frac{c}{d} \right)^2 \quad (47)$$

and  $\Lambda$  is a dimensionless factor the value of which depends upon the shape of the base profile of the airfoil. (See table I and equation (3) of reference 5.) The remaining symbols are defined in Appendix C. Numerical values of the functions of  $M'$  which appear in these equations are given in table II. Experimental pressure distributions can also be corrected by proper modification of the method of reference 5 as indicated in the text.

Tests of an NACA 4412 airfoil at low speed for two ratios of airfoil chord to tunnel diameter demonstrate the validity

of the foregoing equations at low Mach numbers. At angles of attack below the region of maximum lift, the equations are applicable for chord-diameter ratios up to at least 0.625, the maximum ratio tested. In the region of maximum lift a chord-diameter ratio of 0.35 is known to be permissible, and still higher ratios may give satisfactory results. An examination of the validity of the equations at high Mach numbers is not possible at present, but the maximum permissible chord-diameter ratios may be expected to decrease as the Mach number increases.

The tests also indicate that at low Mach numbers the spanwise lift distribution on an airfoil spanning a closed-throat circular tunnel is essentially constant except at angles of attack in the immediate vicinity of the stall. This result corroborates the general conclusion of Appendix B, in which

it is demonstrated that the lift is uniform across an untwisted, constant-chord airfoil spanning any closed-throat wind tunnel, irrespective of the cross-sectional shape of the tunnel.

The correction equations cannot be expected to apply at or in the immediate vicinity of the choking Mach number, which is the maximum Mach number attainable with a given combination of airfoil and tunnel test section. The choking Mach number can be estimated by means of equations given in the report.

AMES AERONAUTICAL LABORATORY,  
NATIONAL ADVISORY COMMITTEE FOR AERONAUTICS,  
MOFFETT FIELD, CALIF.

## APPENDIX A

### TRANSFORMATION OF SERIES OF BESSEL FUNCTIONS

The series involving Bessel functions which appear in the discussions of the interference effects associated with airfoil camber and thickness are, as pointed out in the text, poorly suited for use at small values of the variable  $x$ . It will be shown here, by means of a method demonstrated by Watson (reference 15), that the series may each be expressed as a combination of elementary functions and a convergent power series. The resulting series are well adapted for use in the present problem. The notation used for the Bessel functions is that of Watson (reference 13) and of the Smithsonian Tables (reference 14).

**Series for camber effect.**—The discussion of the interference effects associated with airfoil camber involves the series

$$W_1 = \sum_{s=1}^{\infty} \frac{e^{\lambda_s x} J_1(\lambda_s \eta)}{\lambda_s r J_1(\lambda_s r) J_1''(\lambda_s r)} \quad (\text{A1})$$

convergent for negative values of  $x$ . The summation with respect to  $s$  extends over all the positive roots of the equation

$$J_1'(\lambda_s r) = 0 \quad (\text{A2})$$

Letting  $j_s = \lambda_s r$  and  $\kappa = -x$ , the series may be written

$$W_1 = \sum_{s=1}^{\infty} \frac{J_1(j_s \eta/r)}{j_s J_1(j_s) J_1''(j_s)} e^{-j_s \kappa/r} \quad (\text{A3})$$

where the summation is taken over all the positive roots of the equation

$$J_1'(j_s) = 0 \quad (\text{A4})$$

Now, consider the function

$$-\frac{\pi}{2} \frac{J_1'(w) Y_1(w \eta/r) - J_1(w \eta/r) Y_1'(w)}{J_1'(w)} e^{-w \kappa/r} \quad (\text{A5})$$

where the quantity  $Y_1$  is a Bessel function of the second kind of order unity. This function has a simple pole at each of the points  $w = \pm j_s$  and is one-valued and analytic at all other points in the complex  $w$ -plane. Its residue at the point  $j_s$  can be shown to be

$$\frac{J_1(j_s \eta/r)}{j_s J_1(j_s) J_1''(j_s)} e^{-j_s \kappa/r}$$

which is identical with the general term of the series (A3). By the theorem of residues, the integral of the function (A5) taken counterclockwise around a contour inclosing the portion of the complex plane to the right of the imaginary axis is then equal to  $2\pi i W_1$ . The integral along a large semicircle on the right of the imaginary axis tends to zero when the radius of the semicircle tends to infinity through values such that the semicircle avoids the poles of the integrand. It is thus necessary to retain only the integral along the imaginary axis. The contour must, however, have an in-

dentation to the right of the origin, since the integrand has a pole there with residue  $(r^2 + \eta^2)/r\eta$ . If the radius of the indentation is made to approach zero,  $W_1$  may finally be written

$$W_1 = -\frac{r^2 + \eta^2}{2r\eta} - \frac{1}{2\pi i} \int_{-\infty i}^{\infty i} \left(-\frac{\pi}{2}\right) \frac{J_1'(w) Y_1(w \eta/r) - J_1(w \eta/r) Y_1'(w)}{J_1'(w)} e^{-w \kappa/r} dw \quad (\text{A6})$$

From the known relations for the modified Bessel functions, it is readily shown that

$$\left. \begin{aligned} J_1(\pm it) &= \pm i I_1(t) \\ Y_1(\pm it) &= -I_1(t) \pm \frac{2}{\pi} i K_1(t) \\ J_1'(\pm it) &= I_1'(t) \\ Y_1'(\pm it) &= \pm i I_1'(t) + \frac{2}{\pi} K_1'(t) \end{aligned} \right\} \quad (\text{A7})$$

where  $I_1$  and  $K_1$  are modified Bessel functions of the first and second kind of order unity. By writing the integral in equation (A6) in two parts, one along the positive and one along the negative imaginary axis, and replacing  $w$  in these integrals by  $+it$  and  $-it$ , respectively,  $W_1$  then becomes

$$W_1 = -\frac{r^2 + \eta^2}{2r\eta} + \frac{1}{\pi} \int_0^{\infty} \frac{I_1'(t) K_1(t \eta/r) - I_1(t \eta/r) K_1'(t)}{I_1'(t)} \sin(t \kappa/r) dt$$

or

$$W_1 = -\frac{r^2 + \eta^2}{2r\eta} + \frac{1}{\pi} \int_0^{\infty} K_1(t \eta/r) \sin(t \kappa/r) dt - \frac{1}{\pi} \int_0^{\infty} \frac{K_1'(t)}{I_1'(t)} I_1(t \eta/r) \sin(t \kappa/r) dt \quad (\text{A8})$$

The value of the first integral in this equation is given by Watson in reference 15 as

$$\int_0^{\infty} K_1(t \eta/r) \sin(t \kappa/r) dt = \frac{\pi r \kappa}{2\eta \sqrt{\eta^2 + \kappa^2}} \quad (\text{A9})$$

The second integral can be evaluated by expanding the product  $I_1(t \eta/r) \sin(t \kappa/r)$  in ascending powers of  $t$  and integrating term by term. The series expansion for the product is

$$I_1(t \eta/r) \sin(t \kappa/r) = \sum_{k=0}^{\infty} \sum_{p=0}^{\infty} \frac{(-1)^p t^{2(k+p+1)} \eta^{2k+1} \kappa^{2p+1}}{k! (k+1)! (2p+1)! 2^{2k+1} r^{2(k+p+1)}}$$

and the term-by-term integration gives

$$\int_0^{\infty} \frac{K_1'(t)}{I_1'(t)} I_1(t \eta/r) \sin(t \kappa/r) dt = \pi \sum_{k=0}^{\infty} \sum_{p=0}^{\infty} \frac{(-1)^p \mu'_{2(k+p+1)} \eta^{2k+1} \kappa^{2p+1}}{k! (k+1)! (2p+1)! 2^{2k+1} r^{2(k+p+1)}} \quad (\text{A10})$$

The coefficient  $\mu'_{2(k+p+1)} = \mu'_{2f}$  is given by

$$\mu'_{2f} = \frac{1}{\pi} \int_0^\infty \frac{K_1'(t)}{I_1'(t)} t^{2f} dt$$

which may be written after integration by parts

$$\mu'_{2f} = -\frac{1}{(2f+1)\pi} \int_0^\infty \frac{t^{2f-2} (1+t^2)}{[I_1'(t)]^2} dt \quad (A11)$$

This integral is a constant for any given value of  $f$ .

Reverting to the original variable  $x$ , the expansion for  $W_1$  may finally be written

$$W_1 = -\frac{r^2 + \eta^2}{2r\eta} - \frac{rx}{2\eta\sqrt{\eta^2 + x^2}} + \sum_{k=0}^\infty \sum_{p=0}^\infty \frac{(-1)^p \mu'_{2(k+p+1)} \eta^{2k+1} x^{2p+1}}{k!(k+1)!(2p+1)! 2^{2k+1} r^{2(k+p+1)}} \quad (A12)$$

This agrees with the result given without derivation by Tani and Taima (reference 18).

For purposes of computation the coefficient  $\mu'_{2f}$  is written

$$\mu'_{2f} = -\frac{1}{2(f+1)} [\beta'_{2(f-1)} + \beta'_{2f}] \quad (A13)$$

where

$$\beta'_{2f} = \frac{1}{\pi} \int_0^\infty \frac{t^{2f} dt}{[I_1'(t)]^2} \quad (A14)$$

The quantity  $\beta'_{2f}$  can then be expressed in a form suitable for computation by means of a method devised by Watson for an analogous integral (reference 15).

As the first step, the function

$$\frac{t^{2f}}{[I_1'(t)]^2 \cos(\pi t/b)} \quad (A15)$$

is written as a sum of partial fractions,  $b$  being a positive constant which will be fixed later. This can be accomplished by considering the integral

$$\int \frac{w^{2f} dw}{(w-t)[I_1'(w)]^2 \cos(\pi w/b)} \quad (A16)$$

around the circle  $|w|=R$  in the complex plane. The integrand of the integral (A16) has poles at the points

$$w=t, \quad w=\pm ij_s, \quad w=\pm(n+1/2)b$$

where  $j_s$  is a positive zero of  $J_1'(w)$ ; and  $s=1, 2, 3, \dots, n=0, 1, 2, 3, \dots$ . The residue at the simple pole at  $w=t$  is the function (A15). The residues at the simple poles at  $w=\pm(n+1/2)b$  are

$$-\frac{(-1)^n(n+1/2)^{2f} b^{2f+1}}{\pi(nb+b/2 \mp t)[I_1'(nb+b/2)]^2}$$

The poles at  $w=\pm ij_s$  are second order poles; the residues there are

$$-\frac{(-1)^f j_s^{2f+3}}{J_1^2(j_s)(1-j_s^2)^2 \cosh(\pi j_s/b)} \left[ \frac{j_s}{(j_s \pm it)^2} - \frac{2f - (\pi j_s/b) \tanh(\pi j_s/b) + \frac{3-j_s^2}{1-j_s^2}}{j_s \pm it} \right]$$

Now, the integral (A16) taken around the circle  $|w|=R$  tends to zero when  $R$  tends to infinity in such a manner that the circle never passes through a pole of the integrand. It follows from the theorem of residues that the sum of the residues of the integrand at all its poles is zero; thus

$$\frac{t^{2f}}{[I_1'(t)]^2 \cos(\pi t/b)} = \frac{2}{\pi} \sum_{n=0}^\infty \frac{(-1)^n (n+1/2)^{2f+1} b^{2f+2}}{[(nb+b/2)^2 - t^2][I_1'(nb+b/2)]^2} + 2(-1)^f \sum_{s=1}^\infty \frac{j_s^{2f+4}}{J_1^2(j_s)(1-j_s^2)^2 \cosh(\pi j_s/b)} \left[ \frac{j_s^2 - t^2}{(j_s^2 + t^2)^2} - \frac{2f - (\pi j_s/b) \tanh(\pi j_s/b) + \frac{3-j_s^2}{1-j_s^2}}{j_s^2 + t^2} \right] \quad (A17)$$

By multiplying this equation by  $\cos(\pi t/b)$  and integrating from  $-\infty$  to  $+\infty$ , it can be shown with the aid of certain integral relations given by Watson (reference 15, p. 36) that

$$\int_{-\infty}^\infty \frac{t^{2f} dt}{[I_1'(t)]^2} = 2 \sum_{n=0}^\infty \frac{(n+1/2)^{2f} b^{2f+1}}{[I_1'(nb+b/2)]^2} + 2\pi(-1)^f \sum_{s=1}^\infty \frac{j_s^{2f+3} e^{-\pi j_s/b}}{J_1^2(j_s)(1-j_s^2)^2 \cosh(\pi j_s/b)} \left[ (\pi j_s/b) - 2f - \frac{3-j_s^2}{1-j_s^2} + (\pi j_s/b) \tanh(\pi j_s/b) \right] \quad (A18)$$

and therefore

$$\beta'_{2f} = \frac{1}{\pi} \int_0^\infty \frac{t^{2f} dt}{[I_1'(t)]^2} = \frac{b}{\pi} \sum_{n=0}^\infty \frac{(nb+b/2)^{2f}}{[I_1'(nb+b/2)]^2} + (-1)^f \sum_{s=1}^\infty \frac{j_s^{2f+3}}{J_1^2(j_s)(1-j_s^2)^2} \left[ \frac{(\pi j_s/b)}{\cosh^2(\pi j_s/b)} - \left( 2f + \frac{3-j_s^2}{1-j_s^2} \right) \frac{e^{-\pi j_s/b}}{\cosh(\pi j_s/b)} \right] \quad (A19)$$

The first series in this equation converges rapidly when  $b$  is large, the second when  $b$  is small. A reasonable compromise for purposes of calculation is to take  $b=1$ .

Equation (A19) with  $b=1$  has been used together with equation (A13) to determine the first four values of the coefficient  $\mu'_{2f}$ . The final results are

$$\left. \begin{aligned} \mu'_2 &= -0.999 \\ \mu'_4 &= -1.627 \\ \mu'_6 &= -9.78 \\ \mu'_8 &= -120.8 \end{aligned} \right\} \quad (A20)$$

Comparable values of  $\mu'_2$  and  $\mu'_4$  to the same number of significant figures are given without derivation in reference 18. The value of  $\mu'_2$  in this latter reference agrees with that of the present paper but  $\mu'_4$  differs by one in the third decimal place. The value given in (A20) has been carefully checked for several values of the parameter  $b$  and appears to be correct. Values of  $\mu'_6$  and  $\mu'_8$  apparently have not previously been computed.

Series for thickness effect.—The series which appears in the discussion of the interference effects associated with airfoil thickness is

$$W_2 = \sum_{s=1}^\infty \frac{e^{\lambda_s r} J_1(\lambda_s \eta)}{J_0^2(\lambda_s r)} \quad (A21)$$

convergent for negative values of  $x$ . The summation with respect to  $s$  extends over all the positive roots of the equation

$$J_1(\lambda_s r) = 0 \tag{A22}$$

Letting  $j_s = \lambda_s r$  and  $\kappa = -x$  as before, the series may be written

$$W_2 = \sum_{s=1}^{\infty} \frac{J_1(j_s \eta / r)}{J_0^2(j_s)} e^{-j_s \kappa / r} \tag{A23}$$

where the summation is taken over the positive roots of

$$J_1(j_s) = 0 \tag{A24}$$

The function

$$\frac{\pi}{2} \frac{J_1(w) Y_1(w \eta / r) - J_1(w \eta / r) Y_1(w)}{J_1(w)} w e^{-w \kappa / r} \tag{A25}$$

has a simple pole at each of the points  $w = \pm j_s$ . Its residue at each of these points can be shown to be identical with the general term of the series (A23). Unlike the function in the previous series, this function is regular at the origin. Integration around the portion of the complex plane to the right of the imaginary axis then gives

$$W_2 = -\frac{1}{2\pi i} \int_{-i\infty}^{i\infty} \frac{\pi}{2} \frac{J_1(w) Y_1(w \eta / r) - J_1(w \eta / r) Y_1(w)}{J_1(w)} w e^{-w \kappa / r} dw \tag{A26}$$

By applying the first two of equations (A7) and combining the integrals along the two halves of the imaginary axis as before, the series becomes

$$W_2 = \frac{1}{\pi} \int_0^{\infty} t K_1(t \eta / r) \cos(t \kappa / r) dt - \frac{1}{\pi} \int_0^{\infty} \frac{K_1(t)}{I_1(t)} t I_1(t \eta / r) \cos(t \kappa / r) dt \tag{A27}$$

The first integral can be evaluated by differentiating relation (A9) with respect to  $\kappa$ . This operation gives

$$\int_0^{\infty} t K_1(t \eta / r) \cos(t \kappa / r) dt = \frac{\pi r^2 \eta}{2(\eta^2 + \kappa^2)^{3/2}} \tag{A28}$$

The second integral can be evaluated as before by expanding the product  $t I_1(t \eta / r) \cos(t \kappa / r)$  in ascending powers of  $t$  and integrating term by term. The series expansion for the product is

$$t I_1(t \eta / r) \cos(t \kappa / r) = \sum_{k=0}^{\infty} \sum_{p=0}^{\infty} \frac{(-1)^p t^{2(k+p+1)} \eta^{2k+1} \kappa^{2p}}{k! (k+1)! (2p)! 2^{2k+1} r^{2k+2p+1}}$$

and the term-by-term integration gives

$$\int_0^{\infty} \frac{K_1(t)}{I_1(t)} t I_1(t \eta / r) \cos(t \kappa / r) dt = \pi \sum_{k=0}^{\infty} \sum_{p=0}^{\infty} \frac{(-1)^p \mu_{2(k+p+1)} \eta^{2k+1} \kappa^{2p}}{k! (k+1)! (2p)! 2^{2k+1} r^{2k+2p+1}} \tag{A29}$$

where the coefficient  $\mu_{2(k+p+1)} = \mu_{2f}$  is given by

$$\mu_{2f} = \frac{1}{\pi} \int_0^{\infty} \frac{K_1(t)}{I_1(t)} t^{2f} dt = \frac{1}{(2f+1)\pi} \int_0^{\infty} \frac{t^{2f} dt}{I_1^2(t)} \tag{A30}$$

Reverting to the original variable  $x$ , the expansion for  $W_2$  may finally be written

$$W_2 = \frac{r^2 \eta}{2(\eta^2 + x^2)^{3/2}} - \sum_{k=0}^{\infty} \sum_{p=0}^{\infty} \frac{(-1)^p \mu_{2(k+p+1)} \eta^{2k+1} x^{2p}}{k! (k+1)! (2p)! 2^{2k+1} r^{2k+2p+1}} \tag{A31}$$

The integral (A30) has been investigated by Watson (reference 15). Its value for any given  $r$  can be computed from the series

$$(2f+1) \mu_{2f} = \frac{1}{\pi} \int_0^{\infty} \frac{t^{2f} dt}{I_1^2(t)} = \frac{b}{\pi} \sum_{n=0}^{\infty} \frac{(nb + b/2)^{2f}}{I_1^2(nb + b/2)} + (-1)^{f-1} \sum_{s=1}^{\infty} \frac{j_s^{2f-1}}{J_2^2(j_s)} \left[ \frac{(\pi j_s / b)}{\cosh^2(\pi j_s / b)} - (2f+1) \frac{e^{-\pi j_s / b}}{\cosh(\pi j_s / b)} \right] \tag{A32}$$

where  $b$  is an arbitrary positive constant. This equation has been used with  $b=1$  to determine the first four values of  $\mu_{2f}$ . The final results are

$$\left. \begin{aligned} \mu_2 &= 0.797 \\ \mu_4 &= 1.200 \\ \mu_6 &= 7.46 \\ \mu_8 &= 96.2 \end{aligned} \right\} \tag{A33}$$

The first two of these values agree to the three decimal places with the two numerical values computed by Watson. The remaining two values have not previously been computed.

## APPENDIX B

### CONSTANCY OF LIFT OVER AN AIRFOIL SPANNING A CLOSED-THROAT TUNNEL

Consider an infinitesimally thin untwisted airfoil of constant chord spanning a closed-throat wind tunnel of arbitrary section. Such an arrangement is shown in figure 10, which is a section of the tunnel as seen from downstream. It is assumed that the flow in the tunnel is nonviscous and that the airfoil therefore has no drag.

Suppose for the time being that the lift varies in some manner across the span of the airfoil. Any such variation will be accompanied by a system of vortices trailing from the airfoil and extending infinitely far downstream. If the usual assumption is made that the trailing vortices are parallel to the axis of the tunnel, the flow pattern in a plane normal to the axis at infinity downstream must be of the nature shown

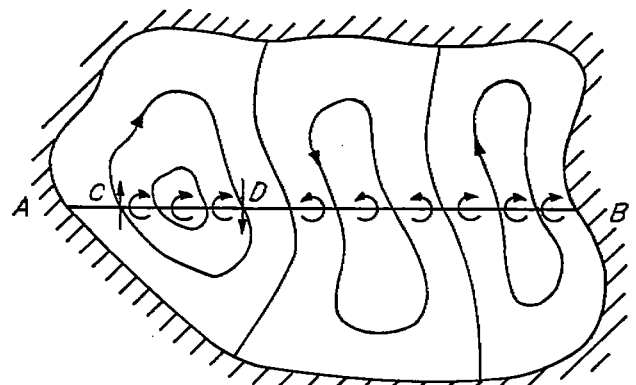


FIGURE 10.—Assumed flow pattern in plane normal to tunnel axis at infinity downstream.

in figure 10. The flow pattern, in general, consists of a number of separate sections within each of which the flow has a closed, circulatory character. The line AB, which represents the projection of the airfoil, extends across every such section, and each of the sections contains the filaments of a portion of the system of trailing vortices. The exact character of the flow pattern in any particular case depends upon the spanwise variation in lift and upon the cross-sectional shape of the tunnel.

Now, consider the flow around a streamline within any one of the separate sections of the flow pattern—say the streamline CD in the section at the left-hand side of the tunnel in figure 10. This streamline, like all the streamlines, intersects the projection AB of the airfoil in two points, denoted as C and D in the figure. The fact that in the presence of the tunnel walls each streamline must intersect AB in two points is essential to the discussion. If it is supposed for purposes of discussion that the direction of flow is clockwise as indicated, the vertical component of velocity at C is upward while the corresponding component at D is downward. This direction of flow corresponds to a net circulation in the clockwise direction for all the trailing vortex filaments enclosed within the streamline.

At the position of the airfoil the pattern of transverse velocities induced by the trailing vortices is geometrically similar to the pattern at infinity downstream, only the magnitude of the velocities being different. Hence, at points on the airfoil directly ahead of point C, the vertical velocity induced by the trailing vortices is upward. At points directly ahead of point D, the velocity is downward. Thus, since the airfoil is untwisted, the airfoil section corresponding to C operates at a larger effective angle of attack than does the section corresponding to D. If the airfoil is of constant chord as assumed, this means that the lift at section C must be greater than the lift at section D.

As has been pointed out, however, the trailing vortices discharged between sections C and D must have a net circulation in the clockwise direction in figure 10. This means that the circulation of the spanwise bound vortices at section D must be greater than at section C. Since the direction of stream flow was taken to be toward the observer, this in turn means that the lift at section C must be less than that at section D, which is in direct contradiction to the previous result. The original supposition that the lift varies across the span thus leads to two mutually contradictory conclusions and is therefore invalid. It follows that the spanwise distribution of lift is uniform across an untwisted, constant-chord airfoil spanning any closed-throat wind tunnel, irrespective of the cross-sectional shape of the tunnel.

As mentioned at the outset, this result depends upon the assumption that the airfoil is infinitesimally thin and has no drag. It will not be strictly true if the increase in effective stream velocity caused by the interference between the walls and the airfoil thickness and wake is not uniform across the span. The result also neglects any effect that the boundary layer along the walls of the tunnel may have upon the lift distribution. That these approximations are not serious, at least in the case of the circular tunnel, is indicated by the experimental results of figures 6 and 7.

The foregoing reasoning is, of course, inapplicable for an airfoil which does not span the tunnel or for a finite-span airfoil in free air. In these instances, the projection of the airfoil does not extend across all of the sections into which the transverse flow pattern is divided, and the streamlines of this pattern need not intersect the projection of the airfoil in two points. Under these conditions a type of varying lift distribution can be found which does not lead to a logical inconsistency.

## APPENDIX C

### LIST OF IMPORTANT SYMBOLS

$c$	airfoil chord
$d$	diameter of circular tunnel
$r$	radius of circular tunnel
$h$	height of rectangular tunnel
$h_1$	height of rectangular tunnel equivalent to circular tunnel with regard to camber effect
$h_2$	height of rectangular tunnel equivalent to circular tunnel with regard to thickness effect
$\tau$	$1/4 \left(\frac{c}{h}\right)$ ; chord-height factor with regard to wake effect in rectangular tunnel
$\tau_2$	$0.321 \left(\frac{c}{d}\right)$ ; chord-diameter factor with regard to wake effect in circular tunnel
$\sigma$	$\frac{\pi}{48} \left(\frac{c}{h}\right)^2$ ; chord-height factor with regard to camber and thickness effect in rectangular tunnel
$\sigma_1$	$0.289 \left(\frac{c}{d}\right)^2$ ; chord-diameter factor with regard to camber effect in circular tunnel
$\sigma_2$	$0.339 \left(\frac{c}{d}\right)^2$ ; chord-diameter factor with regard to thickness effect in circular tunnel
$\Lambda$	factor depending upon shape of base profile (see equation (44) and table I)
$\alpha$	angle of attack
$c_l$	section lift coefficient
$c_{m, c/4}$	section quarter-chord-moment coefficient
$c_d$	section drag coefficient
$V$	stream velocity
$q$	dynamic pressure
$M$	Mach number
$R$	Reynolds number
$x, y, z$	rectangular space coordinates
$x, \omega, \theta$	cylindrical space coordinates (see equations (1))
$\Gamma'$	circulation of single line vortex in tunnel
$d\Gamma'/d\xi$	circulation per unit chord length
$\eta, \zeta$	$y$ and $z$ coordinates of elementary vortex
$\omega_0, \theta_0$	radial and angular coordinates of elementary vortex
$\xi$	chordwise coordinate of elementary vortex; also variable of integration in equations (2) and (3)
$\phi$	velocity potential
$v_x', v_z'$	$x$ and $z$ components of induced velocity
$\Delta V'$	increase in axial velocity at position of airfoil in tunnel
$\mu$	doublet strength
$t_p$	projected thickness of airfoil
$t_e$	effective thickness of airfoil



TABLE II.—COMPRESSIBILITY FACTORS FOR CORRECTION EQUATIONS

$M'$	$\frac{1}{[1-(M')^2]^{1/2}}$	$\frac{1}{[1-(M')^2]}$	$\frac{1}{[1-(M')^2]^{3/2}}$	$\frac{1-0.7(M')^2}{[1-(M')^2]^{3/2}}$	$\frac{1+0.2(M')^2}{[1-(M')^2]^{3/2}}$	$\frac{1+0.4(M')^2}{[1-(M')^2]^{3/2}}$	$\frac{2-(M')^2}{[1-(M')^2]^{3/2}}$	$\frac{8-0.6(M')^2}{[1-(M')^2]^{3/2}}$	$\frac{1-0.7(M')^2[1+0.4(M')^2]}{1-(M')^2}$	$\frac{1+0.2(M')^2[1+0.4(M')^2]}{1-(M')^2}$	$\frac{2-(M')^2[1+0.4(M')^2]}{1-(M')^2}$
0.200	1.021	1.042	1.068	1.033	1.072	1.080	2.084	3.164	1.020	1.067	2.074
.300	1.048	1.099	1.152	1.079	1.173	1.194	2.200	3.394	1.067	1.159	2.174
.400	1.091	1.191	1.299	1.154	1.341	1.382	2.390	3.772	1.125	1.307	2.331
.500	1.155	1.353	1.540	1.270	1.617	1.694	2.694	4.389	1.210	1.540	2.556
.550	1.197	1.454	1.717	1.358	1.821	1.925	2.914	4.830	1.267	1.705	2.723
.600	1.250	1.563	1.958	1.461	2.094	2.234	3.203	5.437	1.337	1.916	2.931
.625	1.281	1.641	2.102	1.527	2.266	2.430	3.383	5.814	1.379	2.046	3.054
.650	1.316	1.732	2.279	1.606	2.471	2.644	3.595	6.258	1.426	2.195	3.193
.675	1.355	1.837	2.489	1.696	2.716	2.943	3.845	6.788	1.479	2.369	3.354
.700	1.400	1.961	2.746	1.804	3.015	3.284	4.146	7.430	1.541	2.575	3.541
.725	1.452	2.108	3.061	1.936	3.332	3.704	4.513	8.217	1.613	2.819	3.761
.750	1.512	2.286	3.456	2.095	3.845	4.234	4.968	9.201	1.697	3.115	4.025
.775	1.582	2.504	3.962	2.297	4.438	4.914	5.545	10.46	1.800	3.478	4.340
.800	1.667	2.778	4.630	2.556	5.222	5.815	6.290	12.11	1.920	3.936	4.745
.820	1.747	3.052	5.333	2.823	6.050	6.787	7.080	13.85	2.050	4.395	5.142
.840	1.843	3.397	6.260	3.168	7.143	8.026	8.103	15.13	2.204	4.970	5.637
.860	1.960	3.840	7.526	3.630	8.639	9.753	9.486	16.24	2.400	5.712	6.272
.880	2.105	4.433	9.333	4.273	10.78	12.22	11.44	28.66	2.659	6.705	7.116
.900	2.294	5.263	12.08	5.229	14.03	15.99	14.37	30.36	3.018	8.098	8.293
.910	2.412	5.817	14.03	5.897	16.36	18.68	16.44	35.12	3.255	9.026	9.078
.920	2.552	6.511	16.61	6.770	19.43	22.24	19.16	41.40	3.552	10.19	10.05
.930	2.721	7.402	20.14	7.946	23.62	27.10	22.86	49.96	3.931	11.69	11.31